ACS OMEGA

Open Access

http://pubs.acs.org/journal/acsodf

Article

Stability and Bonding Analyses of Heteronuclear 1,2-Dichloro-Silylene-Germylenes Supported by Homo/Heterobileptic Donor Base Ligands

Maria Francis, Farsana Abdul Salam, and Sudipta Roy*

Cite This: https://doi.org/10.1021/acsomega.4c04196

Read Online

ACCESS | Metrics & More | Article Recommendations | Supporting Information

ABSTRACT: Herein, we depict the detailed computational studies on the stability and chemical bonding of heteronuclear 1,2-dichloro-silylene-germylenes [(Cl)SiGe(Cl)] supported by homoleptic [L = L′ = cAAC^{Me}; NHC^{Me}; and PMe$_3$] and heterobileptic [L, L′ = cAAC^{Me}; NHC^{Me}; cAAC^{Me}, PMe$_3$; NHC^{Me}; and PMe$_3$] donor base ligands with the general formula (L)(Cl)SiGe(Cl)(L′) having tunable binding energies. The bonding of the corresponding didehalogenated analogue, (L)SiGe(L′) has been also investigated to explore the possibility of multiple bonding between the two-coordinate heteroatoms, Si and Ge. Our studies employing density functional theory, atoms in molecules analysis, and energy decomposition analysis coupled with natural orbitals for chemical valence (EDA-NOCV) unveiled the synthetic viability of the hypothetical compounds in the presence of phosphines and/or stable singlet carbenes, e.g., cyclic alkyl(amino) carbenes (cAACs), and N-heterocyclic carbenes (NHCs) as the suitable ligands. Comparison of the computed bond parameters of the presently hypothesized molecules with those of the relevent experimentally isolated molecules could rationalize the feasibility of the future isolation of the predicted compounds.

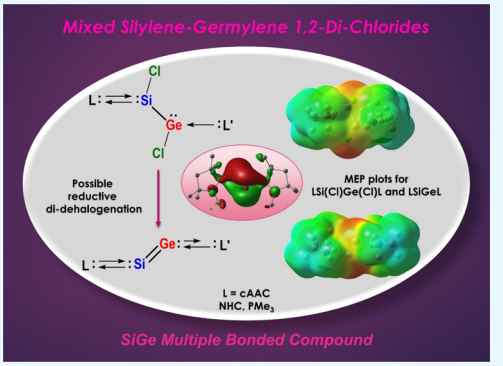

INTRODUCTION

The synthesis and isolation of homo- and heteronuclear diatomic heavier group 14 compounds stabilized by bulky aryl groups or donor base ligands have received great attention over the past years.[1−4] In 2013, Roesky and co-workers reported the first successful solid-state isolation of a cyclic alkyl(amino) carbene (cAAC)-supported dichloro-1,4-diamino-2,3-disila-1,3-butadiene derivative (Figure 1, **A**) with formal C$_{cAAC}$═Si bonds.[4b] In 2014, the same group had utilized compound **A** as the precursor for the isolation of the corresponding cAAC-supported heavier alkene analogue, disila-dicarbene (Figure 1, **B**), featuring the Si═Si bond comprising the two-coordinate Si atoms with a *trans*-bent geometry by the reductive didehalogenation of **A**.[4c] The isolation of the N-heterocyclic carbene (NHC) analogue of compound **B** had been previously reported by Robinson and co-workers in 2008.[4d] In this context, it is notable to mention the earlier groundbreaking discoveries of the homonuclear stable digermene by Lappert,[5,6] and disilene by West,[7] followed by a wide array of other heavier alkenes (R$_2$E = ER$_2$, E = Si, Pb) featuring three-coordinate multiple bonded heavier group 14 elements.[1−4] Similarly, isolation of the previously hypothesized[8] heavier alkyne analogues (RE≡ER, E = Si, Ge, Sn, and Pb), reported by the groups of Power (Figure 1, **C**)[9] and Sekiguchi (Figure 1, **D**)[10] featuring heavier two-coordinate group 14 elements with *trans*-bent geometry are notable. However, the synthetic routes for stabilizing the heavier heteronuclear dichloro-alkenes (R(Cl)E═E′(Cl)R) and the corresponding two-coordinate didehalogenated alkene (RE═E′R) analogues with E = Si, E′ = Ge are extremely rare in the literature. So far, only a very few of the cyclic[11−14] and acyclic[15−17] sila-germenes have been successfully synthesized, and in most of the cases, the stabilization of such species has been achieved by introducing the bulky aryl or other organic substituents at the heavier group 14 elements and thereby featuring the comparatively higher coordination number. In 1991, Baines reported the initial synthesis of tetra-mesityl-germasilene (Figure 1, **E**) with multiple bonded three-coordinate Ge and Si atoms by the photolysis of hexa-mesitylcyclogermadisilane. However, the compound could not be isolated in the solid state.[18]

Over the past few decades, the utilization of donor base ligands, such as NHCs and cAACs, has significantly increased in synthetic main group chemistry for stabilizing exotic molecules with low-coordinate main group elements. A noteworthy contribution in this field has been made by the group of Scheschkewitz, who reported the first instance of the isolation of the monomeric base-stabilized vinylidene analogue,

Received: May 2, 2024
Revised: December 3, 2024
Accepted: December 5, 2024

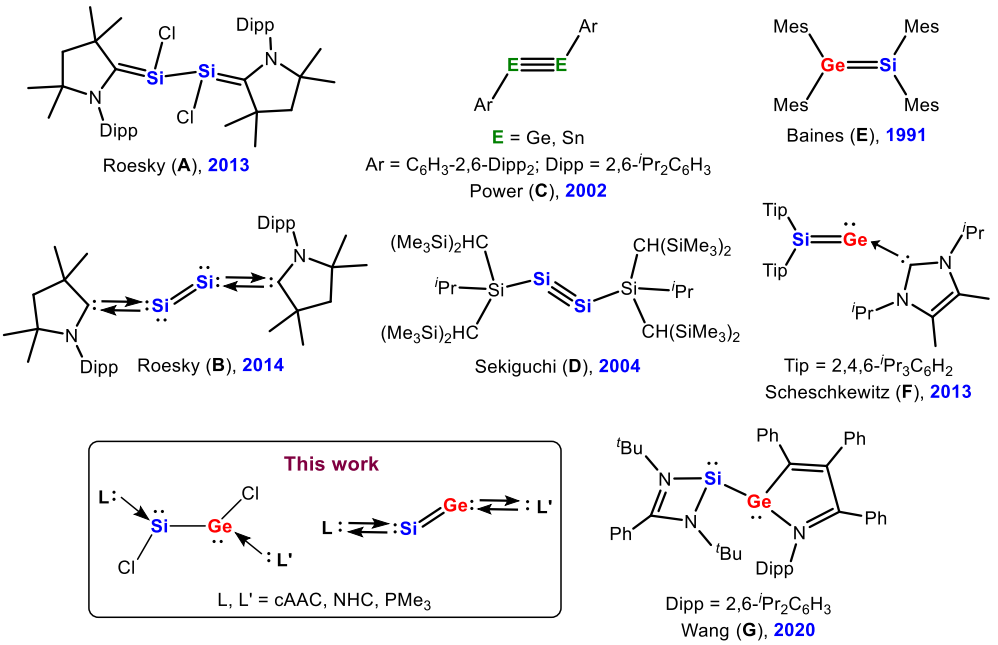

Figure 1. Representative group 14 homo/heteronuclear dichloro-tetrelenes and tetrylenes isolated in the laboratory.

the NHC-stabilized silagermenylidenes (Figure 1, **F**).[19] The subsequent low-temperature reduction of **F** using $\{(^{Mes}NacNac)Mg\}_2$ (NacNac = β-diketiminate) led to the formation of a chloro-silylene intermediate, resulting in the formation of a heteronuclear species featuring the sila-germylene (SiGe) motif.[19] The first interconnected isolable heteronuclear silylene-germylene **G** (Figure 1) was reported by Wang and co-workers in 2020, which demonstrates a *gauche*-bent geometry with the silylene (Si:) and germylene (Ge:) units connected by a Si−Ge single bond.[20] However, there have been no experimental or computational reports so far on the existence of donor base-stabilized heteronuclear 1,2-dichloro-silylene-germylenes, which could further serve as the potential precursors for the corresponding didehalogenated species, sila-germene, featuring the possible multiple bonded two-coordinate Si═Ge moiety. With the discoveries of NHCs by Arduengo[21] and cAACs by Bertrand,[22] the syntheses of various exotic multiple-bonded heavier main-group elements have experienced the landmark success due to their remarkable σ-donation and π-acceptance properties over the traditional phosphine ligands. Based on that evidence, we aimed to computationally predict the stability of a series of hypothetical heteronuclear dichloro-tetrelenes featuring low-coordinate Si and Ge atoms. Herein, we report on the detailed computational studies on stability and chemical bonding of homo/heterobileptic donor base ligand-supported 1,2-dichloro-silylene-germylenes with the general formula (L)Si(Cl)Ge(Cl)(L′) [L, L′ = neutral donor base ligands, e.g., cAAC, NHC, and phosphines; L, L′ = $cAAC^{Me}$ (**1**); L = $cAAC^{Me}$, L′ = NHC^{Me} (**2**); L = $cAAC^{Me}$, L′ = PMe_3 (**3**); L = PMe_3, L′ = $cAAC^{Me}$ (**3′**); L = NHC^{Me}, L′ = $cAAC^{Me}$ (**4**); L, L′ = NHC^{Me} (**5**); L = NHC^{Me}, L′ = PMe_3 (**6**); L = PMe_3, L′ = NHC^{Me} (**6′**); and L, L′ = PMe_3 (**7**)] by using density functional theory (at BP86/def2-TZVPP level of theory), atoms in molecules (AIM) analyses (at the BP86/def2-TZVPP level of theory), and energy decomposition analysis (EDA) coupled with natural orbitals for chemical valence (EDA-NOCV) at the BP86-D3(BJ)/def2-TZV2P level of theory. Further, we studied the effect of introducing the two chloride ligands replacing cAAC (L′) at the Ge (**8**) and Si (**9**) centers on the overall bonding of the respective molecules. We also studied the stability and chemical bonding of the corresponding didehalogenated compound **10** with the general formula (L)SiGe(L′) (L = L′ = cAAC) featuring multiple bonded two-coordinate Si/Ge centers.

RESULTS AND DISCUSSION

Computational Methods. The geometries of the predicted compounds **1**−**7** (Scheme 1) with general formula L−Si(Cl)Ge(Cl)−L′ (L, L′ = $cAAC^{Me}$ (**1**); L = $cAAC^{Me}$, L′ = NHC^{Me} (**2**); L = $cAAC^{Me}$, L′ = PMe_3 (**3**); L = PMe_3, L′ = $cAAC^{Me}$ (**3′**); L = NHC^{Me}, L′ = $cAAC^{Me}$ (**4**); L, L′ = NHC^{Me} (**5**); L = NHC^{Me}, L′ = PMe_3 (**6**); L = PMe_3, L′ = NHC^{Me} (**6′**); and L, L′ = PMe_3 (**7**)), compounds **8**−**9** (Scheme 1) with general formula $L_2Si-GeL'_2$ (L = cAAC; L′ = Cl (**8**); and L = Cl; L′ = cAAC (**9**)), and the didehalogenated analogue (L)SiGe(L′) **10** (L = L′ = cAAC) (Scheme 1) are optimized at BP86/def2-TZVPP[23] levels of theory using Gaussian 09.[24]

We conducted our calculations with dispersion corrections considered in all the cases. To analyze the molecular properties, such as Wiberg bond indices (WBI),[25] occupation numbers (ON), partial charges (q) on the atoms, and the natural bond orbitals, we utilized the NBO 6.0[26] program at the BP86/def2-TZVPP level of theory. The quantum theory of atoms in molecule (QTAIM)[27] is employed to assess the features of the L−Si, Si−Ge, and Ge−L′ bonds. By conducting a topological analysis of the Laplacian of the electron density, one can gain valuable insights into the electronic and conformational properties of the molecules, as well as the interatomic interactions. The wave functions for the QTAIM studies were computed at the BP86/def2-TZVPP level of theory on the optimized geometries of **1**−**10**.

The ADF 2020.102 software package[28a] was utilized to perform the EDA[28b−d] coupled with natural orbitals for chemical valence[28e,f] computations. All these calculations were conducted on preoptimized geometries at the BP86-D3(BJ)/

https://doi.org/10.1021/acsomega.4c04196
ACS Omega XXXX, XXX, XXX−XXX

Scheme 1. Structures of the Species with General Formula (L)(Cl)SiGe(Cl)(L′) (1−7) [L, L′ = cAAC^{Me} (1); L = cAAC^{Me}, L′ = NHC^{Me} (2); L = cAAC^{Me}, L′ = PMe_3 (3); L = NHC^{Me}, L′ = cAAC^{Me} (4); L, L′ = NHC^{Me} (5); L = NHC^{Me}, L′ = PMe_3 (6); L = PMe_3, L′ = cAAC^{Me} (3′); L = PMe_3, L′ = NHC^{Me} (6′); and L, L′ = PMe_3 (7)], 8−9 with General Formula $L_2Si{-}GeL'_2$ [L = cAAC; L′ = Cl (8); L = Cl; L′ = cAAC (9)], and 10 [(cAAC^{Me})SiGe(cAAC^{Me})]

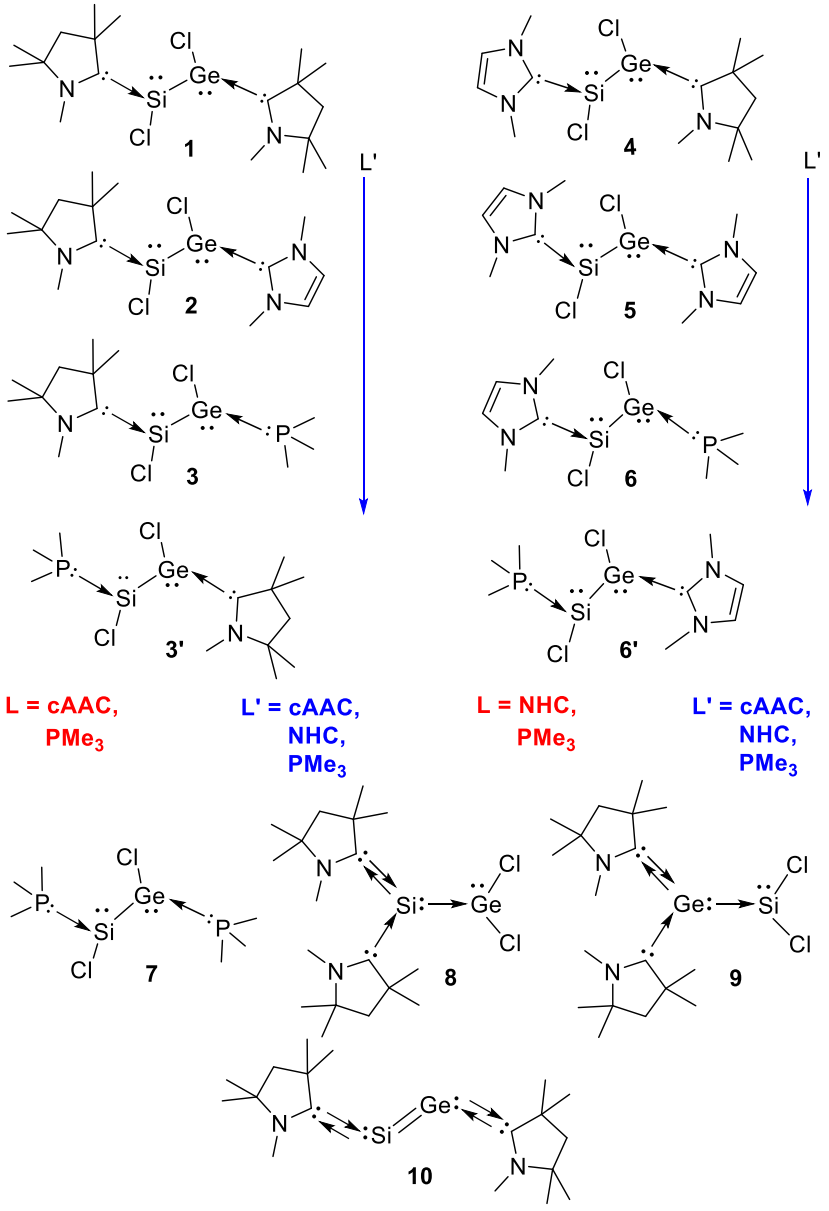

def2-TZV2P level of theory. In the EDA-NOCV approach,[28b−f] the intrinsic interaction energy (ΔE_{int}) between two fragments is decomposed into four energy components as follows

$$\Delta E_{int} = \Delta E_{elstat} + \Delta E_{Pauli} + \Delta E_{orb} + \Delta E_{disp} \quad (1)$$

The interaction energy, ΔE_{int} corresponds to the energy change occurring when the geometrically deformed fragments unite to form the overall complex.[28] ΔE_{elstat} represents the classical electrostatic interaction between the unperturbed charge distributions of fragments in a given geometry, which typically exhibits attractive behavior. ΔE_{Pauli} accounts for Pauli repulsion arising from destabilizing interactions between occupied orbitals, which contributes to steric repulsion. ΔE_{orb} involves orbital interactions between fragments, encompassing bond pair formation, charge transfer, and polarization effects. Finally, the ΔE_{disp} term takes into consideration the attractive dispersion interactions.[28e,f]

For compounds **1−3**, the ligand attached to the Si center (L = cAAC) was kept constant, whereas the ones at the Ge center were varied (L′ = cAAC, NHC, and PMe_3). Similarly, for compounds **4−6**, L is always NHC, and L′ is being varied (cAAC, NHC, and PMe_3, respectively). In compound **7**, the central Si(Cl)Ge(Cl) moiety is flanked by two PMe_3 ligands. The choice of the ligands at the central Si(Cl)Ge(Cl) moiety was made in order to probe the effect of improved σ-donation and π-acceptance properties of the donor base ligands.

Geometry optimizations in the singlet and triplet states were performed for compounds **1−10**, and the results revealed that the singlet state is the electronic ground state (Figure 2). The singlet−triplet energy gaps were found to be in the range of 21.9−36.8 kcal/mol, depicting the stability of the singlet

https://doi.org/10.1021/acsomega.4c04196
ACS Omega XXXX, XXX, XXX−XXX

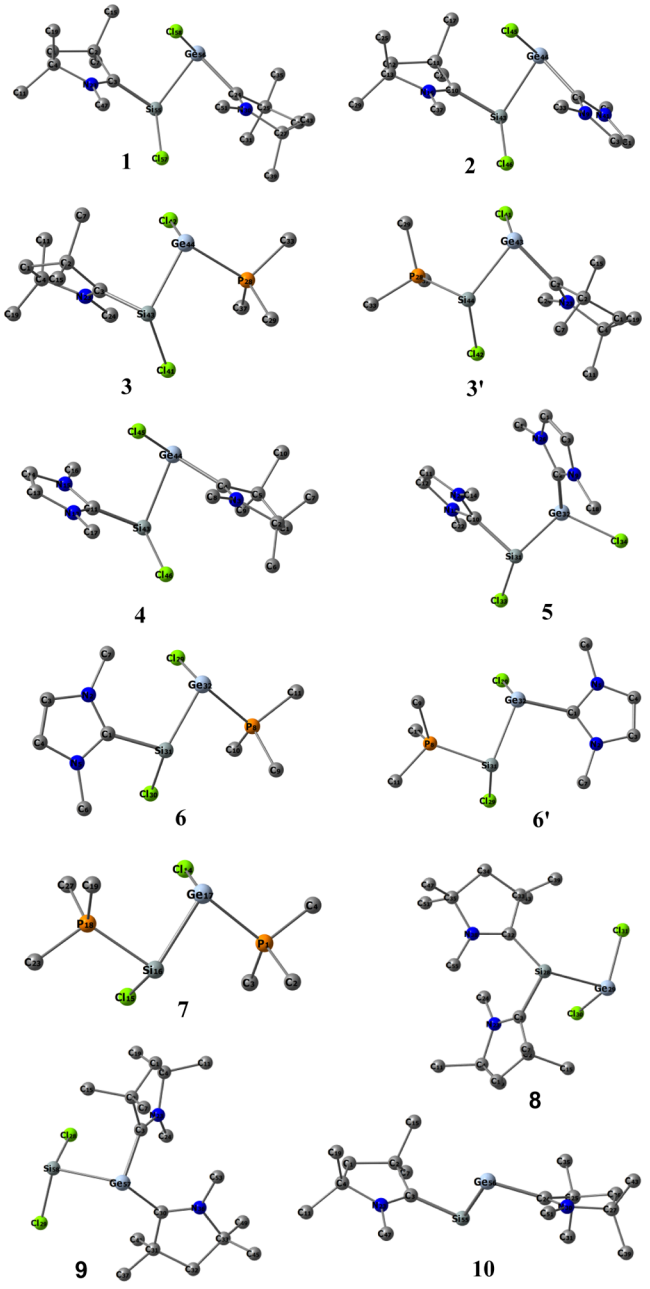

Figure 2. Optimized geometries of compounds **1**−**7** in the singlet ground state with L, L′ = $cAAC^{Me}$ (**1**); L = $cAAC^{Me}$, L′ = NHC^{Me} (**2**); L = $cAAC^{Me}$, L′ = PMe_3 (**3**); L = PMe_3, L′ = $cAAC^{Me}$ (**3′**); L = NHC^{Me}, L′ = $cAAC^{Me}$ (**4**); L, L′ = NHC^{Me} (**5**); L = NHC^{Me}, L′ = PMe_3 (**6**); L = PMe_3, L′ = NHC^{Me} (**6′**); and L, L′ = PMe_3 (**7**); **8**−**9** with general formula $L_2Si{-}GeL'_2$ [L = cAAC; L′ = Cl (**8**); L = Cl; and L′ = cAAC (**9**)]; and **10** [$(cAAC^{Me})SiGe(cAAC^{Me})$] at the BP86/def2-TZVPP level of theory.

ground state. The minima on the potential energy surfaces are made certain in each case by the absence of imaginary frequencies.

The optimized geometries for compounds **1**−**4**, **6**−**7**, and **10** revealed the expected *trans*-bent geometry around the central SiGe backbone. However, we observed the unusual *cis*-geometry in the case of compound **5**, presumably due to the π-stacking interactions between the two five-membered imidazole rings with a $C_{NHC}{-}C_{NHC}$ bond distance of 3.291 Å.[29] Moreover, we found that the plane of cAAC in **3** is almost perpendicular to the plane of the Si−Ge bond (t(NCSiGe) = 80.4°), whereas the plane of NHC in **6** lies in the same plane of the Si−Ge bond (t(NCSiGe) = 1.7°). We assume that the twisting in **3** would have come from stronger steric interactions in the more crowded cAAC ligand at the Si atom.

The computed (at the BP86/def2-TZVPP level of theory) $C_{cAAC}{-}Si$ bond lengths observed in the hypothetical molecules **1**−**3** were found to be 1.881, 1.867, and 1.879 Å, respectively, which are comparable to those of the experimentally isolated compounds, such as (cAAC)SiCl−SiCl(cAAC) (1.823(3) Å/1.826(3) Å)[4b] and (cAAC)SiH−SiH(cAAC) (1.8173(18) Å),[30] but slightly shorter when compared to those reported for (cAAC)SiMe−SiMe(cAAC) (1.8043(12)/1.7977(12) Å).[31] When the Si-bonded ligand changes from cAAC to NHC (**4**−**6**), considerable elongation of the bond length is observed for the $C_{NHC}{-}Si$ bond (1.935 (**4**) Å, 1.935 (**5**) Å, and 1.923 (**6**) Å at BP86/def2-TZVPP). However, no significant change in the bond length was observed when the Ge-bonded ligand was varied. The calculated $C_{NHC}{-}Si$ bond lengths are found to be well in agreement with the laboratory-isolated compounds, such as NHCSi(Cl)═Si(Cl)NHC (1.939(6) Å),[4d] NHC: → $SiCl_4$ (1.928(2) Å),[4d] and NHCSi═SiNHC (1.9271(15) Å),[4d] but slightly shorter than that observed in NHC: → $SiCl_2$ (1.985(4) Å).[32] The $Me_3P{-}Si$ bond length in the hypothetical molecule, calculated at the BP86/def2-TZVPP level of theory is found to be 2.289 Å, which is comparable to that of the experimentally isolated phosphasilanes, such as $(MesPH)_3SiPh$ (2.2749(7)−2.2829(8) Å),[33] and the donor-stabilized thiosilanoic phosphane L′Si-(PH_2)═S [(L′ = CH[(C = CH_2)CMe(NAr)$_2$], Ar = 2,6-^{i}Pr$_2$C$_6$H$_3$)] (2.2400(2) Å).[34] When the Ge-bonded ligand is cAAC (**1** and **4**), the calculated $C_{cAAC}{-}Ge$ bond lengths are found to be 2.022 and 2.002 Å, respectively, which are comparable to those of cAAC-stabilized Ge(I) radicals Cy-cAAC:GeN(SiMe$_3$)Dipp (Dipp = 2,6-^{i}Pr$_2$C$_6$H$_3$) (1.986(2) Å),[35] but slightly shorter than those of cAAC: → $GeCl_2$ (2.1321(16) Å),[36] whereas slightly longer than those observed for cAACGe(Me)−Ge(Me)cAAC (1.9240(17) Å), (1.9069(18) Å),[31] and the acyclic germylones (Me_2-cAAC)$_2$Ge (1.9386(16) Å, 1.9417(15) Å).[36] The calculated $C_{NHC}{-}Ge$ bond lengths found in compounds **2** and **5** are found to be 2.077 and 2.064 Å, respectively, which are comparable to the recently reported phosphinidene-chlorotetrylenes (L)P−GeCl(L′) using cAAC and NHC as the ligands (L = cAAC; L′ = NHC) (2.0857(16) Å)[37] and the reported Ge−C bond lengths in NHC: → $GeCl_2$ (2.110(4) Å),[38] NHCGe = GeNHC (2.030(3) Å),[38] and NHC-stabilized silagermenylidene $NHC^iPr_2Me_2$ → Ge−Si(Tip)$_2$ ($NHC^iPr_2Me_2$ = 1,3-diisopropyl-4,5-dimethylimidazol-2-ylidene, Tip = 2,4,6-^{i}Pr$_3$C$_6$H$_2$) (2.0474(18) Å).[19] The calculated Ge−PMe_3 bond lengths in compounds **3**, **6**, and **7** are found to be 2.417, 2.404, and 2.392 Å, respectively, which are in good agreement with the reported diphosphagermylenes (Dipp)$_2$P$_2$Ge (Dipp = 2,6-^{i}Pr$_2$C$_6$H$_3$) (2.3823(12) Å)[39] and LGeP(H)SiMe$_3$ [L = CH{(CMe)(2,6-^{i}Pr$_2$C$_6$H$_3$N)}$_2$] (2.426(7) Å).[40] The Si−Ge bond length seen in the central moiety of the hypothetical molecules **1**−**7** is in the range of 2.464−2.572 Å, which is well comparable to those reported for the potassium silagermenide ((Xyl)N)CSi$_2$(Tip)$_4$Ge−K-(THF) (Tip = 2,4,6-^{i}Pr$_3$C$_6$H$_2$, Xyl = 2,6-Me$_2$C$_6$H$_3$) (2.4295(10) Å),[41] and the functionalized disilagermirene−nickel complex (Tip)$_2$SiSi(Tip)Ge(PPh$_2$)Ni(NHC)$_2$ (Tip = 2,4,6-^{i}Pr$_3$C$_6$H$_2$, NHC = 1,3-di-isopropyl-4,5-dimethylimidazol-

https://doi.org/10.1021/acsomega.4c04196
ACS Omega XXXX, XXX, XXX−XXX

Table 1. NBO Results of Compounds cAAC^{Me}−Si(Cl)Ge(Cl)−cAAC^{Me} (1), cAAC^{Me}−Si(Cl)Ge(Cl)−NHC^{Me} (2), cAAC^{Me}−Si(Cl)Ge(Cl)−PMe$_3$ (3), NHC^{Me}−Si(Cl)Ge(Cl)−cAAC^{Me} (4), NHC^{Me}−Si(Cl)Ge(Cl)−NHC^{Me} (5), NHC^{Me}−Si(Cl)Ge(Cl)−PMe$_3$ (6), and PMe$_3$−Si(Cl)Ge(Cl)−PMe$_3$ (7) at the BP86-D3(BJ)/def2-TZVPP Level of Theory ON, Polarization, and Hybridization of the L−Si, Si−Ge, and Ge−L′ bonds[a]

compound	bond	ON	polarization and hybridization (%)			WBI	q	
							Si	Ge
1	C3−Si55	1.52	C: 58.7 s(21.33); p(71.45)	Si: 41.3 s(39.6); p(59.6)		0.99	0.511	0.443
		1.46	C: 34.8 s(21.6); p(67.6)	Si: 65.2 s(3.3); p(67.6)				
	Si55−Ge56	1.69	Si: 62.1 s(41.4); p(57.6)	Ge: 37.9 s(4.6); p(94.8)		0.73		
	Ge56−C24	1.92	C: 76.8 s(38.4); p(61.5)	Ge: 23.2 s(9.7); p(89.9)		0.88		
	Ge lone pair	1.84	s(79.7); p(20.2)					
2	C10−Si43	1.93	C: 72.0 s(37.6); p(62.2)	Si: 28.0 s(42.4); p(56.9)		1.03	0.477	0.341
	Si43−Ge44	1.75	Si: 72.2 s(39.6); p(59.6)	Ge: 27.8 s(5.2); p(94.2)		0.76		
	Ge44−C2	1.94	C: 77.4 s(41.9); p(58.1)	Ge: 22.6 s(7.1); p(92.4)		0.76		
	Si lone pair	0.86	s(1.6); p(97.8)					
	Ge lone pair	1.90	s(81.3); p(18.7)					
3	C3−Si43	1.94	C: 75.9 s(40.2); p(59.6)	Si: 24.1 s(15.7); p(83.4)		1.00	0.467	0.185
	Si43−Ge44	1.64	Si: 48.9 s(8.3); p(90.7)	Ge: 51.1 s(9.2); p(90.3)		0.84		
	Ge44−P28	1.93	P: 73.3 s(29.0); p(70.9)	Ge: 26.7 s(5.7); p(93.6)		0.69		
	Si lone pair	1.73	s(69.1); p(30.7)					
	Ge lone pair	1.92	s(82.5); p(17.4)					
4	C11−Si43	1.95	C: 77.0 s(43.3); p(56.5)	Si: 23.0 s(12.0); p(87.0)		0.82	0.371	0.412
	N15−Si43−Ge44	1.38	N: 53.9 s(0.0); p(99.9)	Si: 23.5 s(6.4); p(92.3)	Ge: 22.6 s(6.4); p(93.1)	0.72 (Si−Ge)		
	Ge44−C4	1.93	C: 76.4 s(38.8); p(61.1)	Ge: 23.6 s(11.4); p(88.2)		0.90		
	Si lone pair	1.85	s(73.8); p(26.0)					
	Ge lone pair	1.86	s(78.1); p(21.8)					
5	C10−Si31	1.94	C: 77.5 s(44.1); p(55.7)	Si: 22.5 s(11.6); p(87.3)		0.83	0.325	0.310
	Ge32−C2	1.94	C: 78.2 s(42.8); p(57.2)	Ge: 21.8 s(7.6); p(91.9)		0.75		
	N26−Si31−Ge32	1.42	N: 70.7 s(0.1); p(99.8)	Si: 14.3 s(8.1); p(90.7)	Ge: 15.0 s(15.0); p(93.4)	0.77		
	Si lone pair	1.84	s(71.8); p(28.1)					
	Ge lone pair	1.90	s(81.1); p(18.8)					
6	C1−Si31	1.95	C: 75.6 s(42.9); p(56.9)	Si: 24.4 s(13.7); p(85.2)		1.04	0.247	0.098
	Si31−Ge32	1.85	Si: 51.3 s(13.5); p(85.8)	Ge: 48.7 s(10.5); p(89.1)		0.81		
	Ge32−P8	1.93	P: 72.8 s(29.3); p(70.5)	Ge: 27.2 s(5.8); p(93.4)		0.78		
	Si lone pair	1.75	s(64.0); p(35.8)					
	Ge lone pair	1.90	s(79.2); p(20.7)					
7	P18−Si16	1.94	P: 71.6 s(30.3); p(69.4)	Si: 28.4 s(8.8); p(89.8)		0.85	0.076	0.102
	Si16−Ge17	1.85	Si: 50.5 s(10.3); p(88.5)	Ge: 49.5 s(8.6); p(90.9)		0.96		
	Ge17−P1	1.93	P: 72.9 s(29.4); p(70.5)	Ge: 27.1 s(5.9); p(93.4)		0.79		
	Si lone pair	1.88	s(72.9); p(27.0)					
	Ge lone pair	1.92	s(80.4); p(19.5)					

[a]ON, polarization, and hybridization of the L−Si, Si−Ge, and Ge−L′ bonds.

2-ylidene) (2.432(4), 2.380(4) Å).[42] The Si−Ge bond length is also found to be very close to that of **compound G** (Figure 1, 2.4498(9) Å), which is the first reported example of the experimentally isolated silylene-germylene (Figure 1).[20] For compounds **8**−**9**, it is observed that both the cAAC ligands in L$_2$Si−GeL′$_2$ have slightly different bond lengths (1.857, 1.875 Å (**8**); 1.973, 1.982 Å (**9**)). The Si−Ge bond length is found to be significantly longer than those observed in compounds **1**−**7** (2.667 (**8**) and 2.665 (**9**) Å).

The NBO analysis performed (at the BP86/def2-TZVPP level of theory on the optimized structures) on compounds **1**−**7** provided insight into the electronic structure and bonding (Table 1). We observed two-bond occupancies for the C$_{cAAC}$−Si bond in **1** (1.52 and 1.46), where the first bond was polarized toward the C atom (58.7%) and the second toward the Si atom (65.2%). In compounds **2**−**7**, the L−Si bond was found to have a single occupancy and is polarized toward the respective ligands (71.6−77.5%). This corresponds to σ-donation from the ligand L to the Si atom. On the other hand, backdonation from the Ge center to the attached ligand was not observed in any case, irrespective of the nature of the ligand L′, which in turn supports the presence of a localized lone pair of electrons majorly of s character (∼80%) on Ge featuring the germylene nature (Figure 3, HOMO − 1). The Si−Ge bond pair of electrons were found to be polarized toward the Si atoms in **1** (62.1) and **2** (72.2), whereas the same was found to be equally shared between the Si and Ge atoms for compounds **3**, **6**, and **7**. We performed NBO analysis of the previously isolated molecule ((cAAC)SiCl−SiCl-(cAAC)), **A** (Figure 1),[4b] to compare the results with our calculations. For **A**, there was only single bond occupancy (1.95) observed for the C$_{cAAC}$−Si bonds in contrast to compound **1**, and the bond is polarized toward C$_{cAAC}$. Whereas for the Si−Si bond, two bond occupancies (1.88 and 1.45) were observed with a WBI of 0.94. The HOMO − 1 of **A** is denoted as weakly bonding electrons at the silicon

https://doi.org/10.1021/acsomega.4c04196
ACS Omega XXXX, XXX, XXX−XXX

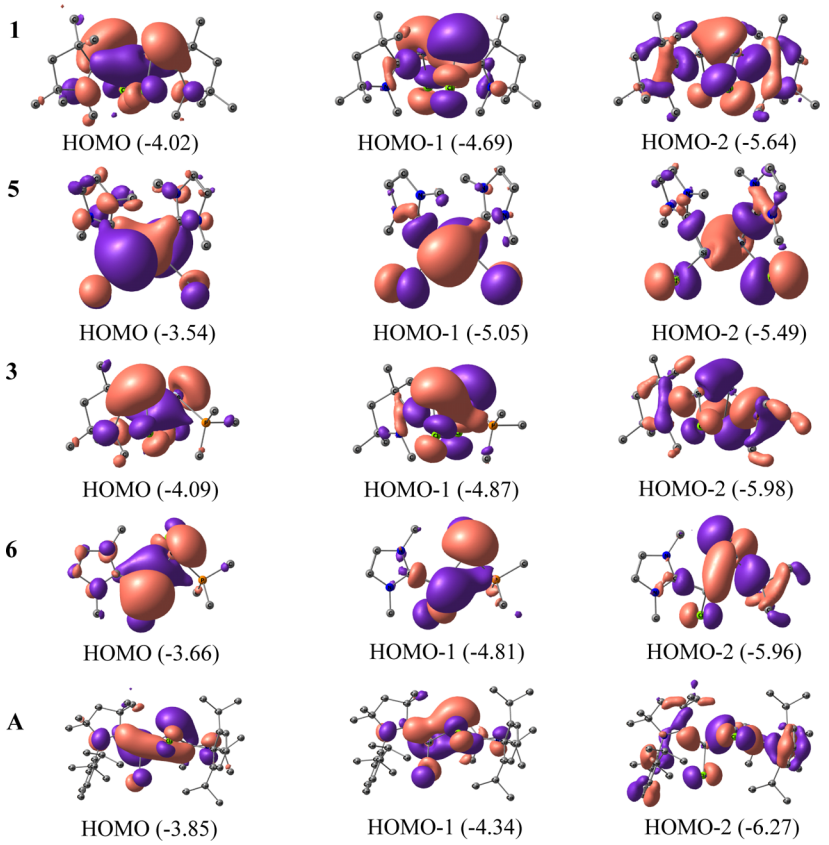

Figure 3. Representative molecular orbitals of hypothetical compounds **1**, **5**, **3**, **6**, and the previously isolated compound **A**, calculated at the BP86/def2-TZVPP level of theory. The values in the parentheses are the energies of the orbitals in eV. See the Supporting Information for the selected molecular orbitals of **1**−**7**.

atoms, which is not observed in the case of compounds **1**−**7** we have chosen for the present study. The existence of the three-centered two-electron bonds (N−Si−Ge) was observed in compounds **4** and **5**, where N is from the ligand L and L′, respectively, in compounds **4** and **5**. In all cases (**1**−**7**), the WBI of the Si−Ge bond is found to be in the range of a single bond (0.72−0.96). The highest WBI of the Si−Ge bond was observed when the ligand was PMe_3 (**7**), and the lowest was observed when the ligands were NHC and cAAC (**4**). The trend of the above WBI is also in line with the calculated bond dissociation energies (BDEs) of the Si−Ge bonds (see the Supporting Information). Varying the ligands at the Ge center did not affect the WBI of the cAAC−Si bond (∼1.0), but a slightly higher WBI was observed in **6**, where the Ge-bonded ligand is PMe_3, and the Si-bonded ligand is NHC. This is also accounted for by the slightly shorter Si−Ge bond lengths observed in **6** than in **4** and **5**. A WBI of <1 and the localized lone pair on the Ge centers eliminate the presence of multiple bonds in these compounds. The nonplanarity of L−Si−Ge−L′ in compounds **1**−**7** disrupts an effective π-conjugation over the $C_LSiGeC_{L'}$ backbone. For compounds **1**−**7**, HOMO comprises the Si lone pair (**2**−**6**) or the π-type Si−cAAC bond (**1**). The HOMO − 1 reveals the σ-type lone pair of Ge, which does not participate in delocalization with the attached ligand (L′). The Si−Ge σ-bond is depicted by the HOMO − 2 (Figure 3). Representative orbitals for compounds **3′** and **6′** have been displayed in the Supporting Information.

Next, a different set of ligands have been chosen at Si and Ge centers to analyze the ligand effect on the bonding nature of the SiGe backbone of the compounds $L_2Si{-}GeL'_2$ (L = cAAC; L′ = Cl (**8**) and L = Cl; L′ = cAAC (**9**)) (Figure 2). The NBO analysis performed on the optimized geometries of **8**−**9** at the BP86/def2-TZVPP level of theory (Figure 4, see the Supporting Information) revealed that the bond between two cAAC units and the Si/Ge backbone in $L_2Si{-}GeL'_2$ are nonidentical; the first bond has single occupancy and is polarized toward C_{cAAC}, whereas the other C_{cAAC}-Si/Ge bond has two bonding occupancy in which the first is polarized toward C and the other toward E (E = Ge (**8**) and E = Si (**9**)).

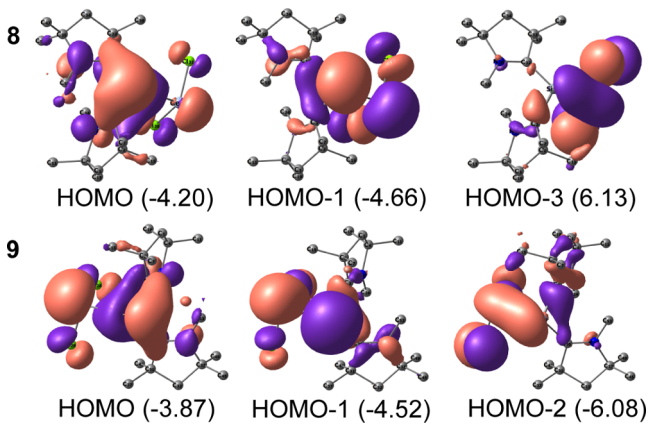

Figure 4. Representative molecular orbitals of compounds **8** and **9** calculated at the BP86/def2-TZVPP level of theory. The values in the parentheses are the energies of the orbitals in eV.

https://doi.org/10.1021/acsomega.4c04196
ACS Omega XXXX, XXX, XXX−XXX

This difference is observed in their bonding occupancies, where the singly occupied bond shows WBI values of 0.97 (**8**) and 0.94 (**9**), and the doubly occupied bond shows slightly higher values of 1.10 (**8**) and 1.32 (**9**). The HOMOs of **8**–**9** show significant π-delocalization over C_{cAAC}–Si/Ge–C_{cAAC} centers. The Si–Ge bond is found to be polarized toward the atom to which cAAC ligands are bonded, and the presence of lone pairs is observed on the atom on which Cl atoms are bonded. From the WBI of the Si–Ge bond, it is clear that the bond has a single bond character and can be visualized in HOMO − 3 and HOMO − 2 of **8** and **9**, respectively. With the quest of finding out the possible ligand fields for stabilizing the multiple bonded silylene-germylene, which might be synthetically achieved by the reductive didehalogenation of the corresponding 1,2-dihalides (**1**–**7**), we optimized the geometry of compound [($cAAC^{Me}$)SiGe($cAAC^{Me}$)] (**10**) at the BP86/def2-TZVPP level of theory (Figure 5). The

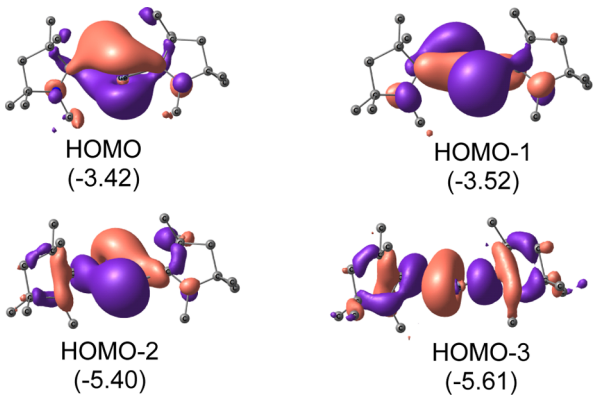

Figure 5. HOMO, HOMO − 1, HOMO − 2, and HOMO − 3 of compound **10** at the BP86/def2-TZVPP level of theory. The values in the parentheses are the energies of the orbitals in eV.

calculated Si–Ge bond length in **10** is found to be 2.331 Å, which is significantly shorter than the SiGe backbone present in parent molecule **1**, implying the formation of multiple bonds between the Si and Ge atoms (Figure 5). The BDEs of the Si–Ge (64.31 kcal/mol) and cAAC–SiGe–cAAC (137.06 kcal/mol) bonds in **10** also show the considerable increase compared to those obtained for **1** (see the Supporting Information). Moreover, the NBO studies also reveal the presence of two bond occupancies between Si and Ge atoms, which can be visualized in HOMO (π-type) and HOMO − 3 (σ-type). The WBI of the Si–Ge bond in compound **10** (**1-2Cl**) is 1.4, which predicts the partial double bond nature of the Si–Ge bond and slightly lower than the WBI of $cAAC_2Si_2$ (1.53).[43] The lone pair is present on both Si and Ge atoms, which is majorly of s-type and slightly overlaps with the carbene carbon (HOMO − 2, Figure 5).

The NBO results of the heteronuclear compound **10** were concurrent with the experimentally isolated homonuclear compound $cAAC_2Si_2$ (**B**)[4d] revealing a possible isolation of **10**. The presence of the lone pairs on Si atoms and double bond occupancies present for the Si–Si bond are found to be the most common features. A slightly higher WBI was observed in **B** (1.53) compared to that of **10**, probably due to better orbital overlap of the Si atoms.

Next, we performed the QTAIM analyses to assess the features of the L–Si, Si–Ge, and Ge–L′ bonds for the hypothesized molecules **1**–**10** (Figure 6, (a) for compound **1** and (b) for compound **10**; see the Supporting Information for details). By conducting a topological analysis of the Laplacian of the electron density, one can gain valuable insight into the electronic and conformational properties of the molecules as well as the interatomic interactions. The wave functions for the QTAIM studies were computed at the BP86/def2-TZVPP level of theory on the optimized geometries of **1**–**10**. The electron densities ($\rho(r)$) of the L–Si and Ge–L′ bonds in **1**–**10** are in the range of 0.124–0.078. The strength of a chemical bond, indicated by its bond order (BO), is reflected in the electron density at the bond critical point (BCP) ($\rho(r)$). It has been observed that when PMe_3 is bonded to Si or Ge atoms, the electron density ($\rho(r)$) decreases. This finding is consistent with the calculated BDEs (see the Supporting Information) for the respective bonds, as the presence of PMe_3 corresponds to a decrease in BDE. Another parameter that characterizes a bond is the Laplacian of the electron density ($\nabla^2\rho(r)$). Regions exhibiting negative Laplacian of the electron density, $\nabla^2\rho < 0$, indicate a local concentration of electron density. When $\nabla^2\rho < 0$ is observed in the internuclear region, it suggests that the interatomic interaction is shared. The positive Laplacian ($\nabla^2\rho(r)$) at the BCP of the L–Si and Ge–L′ bonds in **1**–**10** indicates the closed-shell interactions. It is observed that the electron densities ($\rho(r)$) of the Si–Ge bonds indicate a weak interaction between the Si and Ge atoms. The highest electron density ($\rho(r)$) is found for **10** (0.079), which is due to the presence of a double bond. In contrast, the lowest electron densities ($\rho(r)$) are observed for **8** and **9** (0.053), primarily attributed to the presence of a dative bond, as also suggested by the EDA-NOCV analyses. Even though $\nabla^2\rho(r)$ is negative for **8** and **9**, it is found to be the least and very close to zero. The negative sign of the Laplacian of the electron density, $\nabla^2\rho(r)$, in the case of Si–Ge bonds, in compounds **1**–**7** and **10** is a clear indication of the covalent nature of the corresponding bonds.

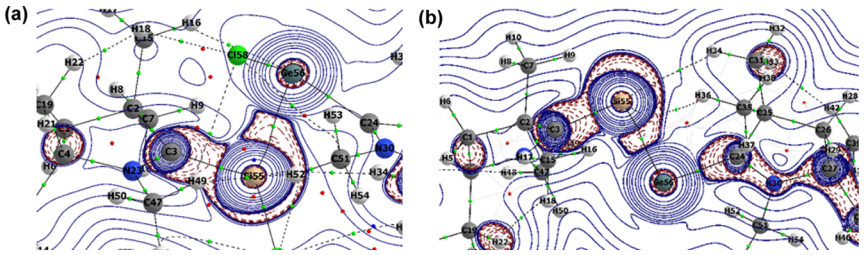

Figure 6. Contour plot of Laplacian distribution [$\nabla^2\rho(r)$] in the C3–Si55–Ge56 plane of **1** (a) and **10** (b). Solid blue lines indicate the areas of charge concentration ($\nabla^2\rho(r) < 0$), while dotted purple lines denote charge depletion ($\nabla^2\rho(r) > 0$). Solid lines connecting atomic nuclei (black) are the bond paths, and green spheres on bond path indicates the BCP. See the Supporting Information for compounds **2**–**9**.

https://doi.org/10.1021/acsomega.4c04196
ACS Omega XXXX, XXX, XXX−XXX

Scheme 2. Left: Possible Bonding Scenarios of Compounds 1−7 (Also See Table S7); (a) Interaction of Neutral Singlet Fragments, Creating a Dative Bond between [L L′] and [Si(Cl)Ge(Cl)]; (b) Interaction of Singly Charged ([L L′]$^+$ and [Si(Cl)Ge(Cl)]$^-$) Doublet Fragments Forming Electron-Sharing σ-Bonds, Dative σ-Bonds, and π-Dative Bonds; (c) Interaction between [L L′]$^{2+}$ and [Si(Cl)Ge(Cl)]$^{2-}$ Fragments in Doubly Charged Triplet States, Forming Electron-Sharing σ-Bonds and π-Dative Bonds; Right: Splitting of Si−Ge Bonds of Compounds 1−7 (d−f); (d) Electron Sharing between Two Doublet Fragments; and (e,f) Charged Fragments in Their Singlet States

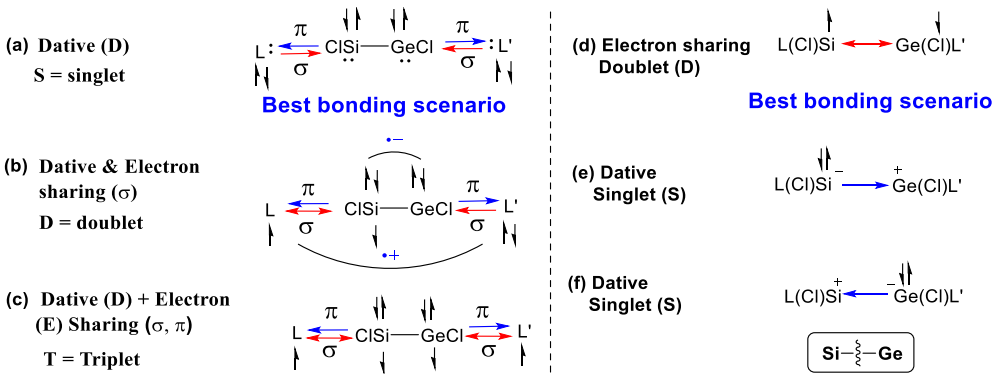

Table 2. EDA-NOCV Analyses of L−Si(Cl)Ge(Cl)−L′ Bonds of Compounds 1−7 (L−Si(Cl)Ge(Cl)−L′) Using [L L′] and [Si(Cl)Ge(Cl)] in the Electronic Singlet (S) States as Interacting Fragments at the BP86-D3(BJ)/TZ2P Level of Theory[a]

energy	interaction	1	2	3	4	5	6	7
ΔE_{int}		−152.9	−142.9	−131.7	−139.0	−114.4	−118.1	−99.6
ΔE_{Pauli}		501.7	484.1	470.6	462.6	415.5	382.7	494.8
ΔE_{ele}		−330.9 (50.5%)	−317.2 (50.6%)	−303.8 (50.4%)	−309.5 (51.4%)	−279.0 (52.6%)	−254.1 (50.7%)	−306.8 (51.6%)
ΔE_{disp}		−32.4 (5.0%)	−29.6 (4.7%)	−30.1 (5.0%)	−29.4 (4.9%)	−20.65 (3.9%)	−23.9 (48%)	−26.3 (4.4%)
ΔE_{orb}		−291.3 (44.5%)	−280.2 (44.7%)	−268.4 (44.6%)	−262.7 (43.7%)	−230.3 (43.5%)	−222.9 (44.5%)	−261.3 (44.0%)
$\Delta E_{orb(1)}$	L → Si(Cl)Ge(Cl) ← L′σ donation	−109.7 (37.64%)	−115.3 (41.1%)	−104.2 (38.8%)	103.6 (39.4%)	−85.3 (37.1%)	−102.4 (45.9%)	−126.1 (48.3%)
$\Delta E_{orb(2)}$	L → Si(Cl)Ge(Cl) ← L′σ donation	−95.5 (32.8%)	−85.3 (30.4%)	−92.4 (34.5%)	−74.6 (28.4%)	−74.0 (32.1%)	−67.0 (30.2%)	−81.0 (31.0%)
$\Delta E_{orb(3)}$	L ← Si(Cl)Ge(Cl) → L′π backdonation	−39.9 (13.7%)	−36.9 (13.1%)	−31.1 (11.6%)	−41.4 (15.7%)	−35.8 (15.6%)	−18.8 (8.4%)	−17.0 (6.5%)
$\Delta E_{orb(4)}$	L ← Si(Cl)Ge(Cl) → L′π backdonation				−9.6 (3.7%)	−9.4 (4.1%)	−9.6 (4.3%)	
$\Delta E_{orb(rest)}$		−46.3 (15.9%)	−42.9 (15.4%)	−40.6 (15.1%)	−33.4 (12.8%)		−25.1 (11.2%)	−37.2 (14.2%)

[a]Energies are in kcal/mol. The values in the parentheses show the contribution to the total attractive interaction $\Delta E_{disp} + \Delta E_{elstat} + \Delta E_{orb}$. The values in parentheses show the contribution to the total orbital interaction ΔE_{orb}.

The ellipticity, ε, measures the π character of a bond. The degree of ε is influenced by the symmetrical or asymmetrical distribution of the electron density in a bond. When a bond has cylindrical symmetry, such as in single and triple bonds, the value of ε is almost zero due to the uniform distribution of electron density along the bond axis. On the other hand, for a double bond, ε is greater than zero because of the uneven distribution of electron density perpendicular to the bond path. The greater value of ε observed for L−Si bonds compared to those for the Ge−L′ bonds suggests the stronger double bond character of the L−Si bonds due to the smaller size of the Si atom and, thus, efficient overlap of orbitals compared to that in the presence of the Ge atom. Conversely, the lower value of ε for the Si−Ge (0.103 to +0.033) indicates the single bond nature for compounds **1**−**7**. Notably, the ε value of the Si−Ge bond increased significantly to 0.324 in **10** (Figure 6, (b)), indicating the double bond nature. This finding is consistent with the results obtained from NBO analysis, which revealed that the Si−Ge bond had two bonding occupancies and a WBI of 1.4.

To have a more accurate picture of the chemical bonding, we further performed the EDA coupled with natural orbitals for chemical valence (EDA-NOCV) at the BP86-D3(BJ)/TZ2P level of theory of the hypothetical compounds **1**−**10**. By using the fragments in the appropriate electronic states, the EDA approach can be used to recommend the optimum bonding description in accordance with the electronic structures. Initially, compounds **1**−**7** (L-Si(Cl)Ge(Cl)-L′) were fragmented into two parts: the ligands [L L′], and the central backbone [Si(Cl)Ge(Cl)]. By changing the charge, and spin states of these fragments, we attempted three bonding possibilities and performed the EDA-NOCV studies. The first bonding possibility was the interaction of neutral singlet fragments, creating a dative bond between [L L′] and [Si(Cl)Ge(Cl)]. The second bonding possibility was the interaction of singly charged ([L L′]$^+$ and [Si(Cl)Ge(Cl)]$^-$) doublet fragments, forming electron-sharing σ-bonds, dative σ-bonds, and π-dative bonds. The third was the interaction between [L L′]$^{2+}$ and [Si(Cl)Ge(Cl)]$^{2-}$ fragments in doubly

https://doi.org/10.1021/acsomega.4c04196
ACS Omega XXXX, XXX, XXX−XXX

cAAC−Si(Cl)Ge(Cl)−cAAC	[(cAAC) (cAAC)] (S)	[Si(Cl)Ge(Cl)] (S)
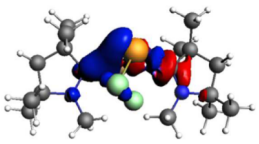 $\Delta\rho_{(1)}$ $\Delta E_{orb(1)}$ = -109.66; $\lvert\nu_{1\alpha}/\nu_{1\beta}\rvert$ = 0.57/0.57	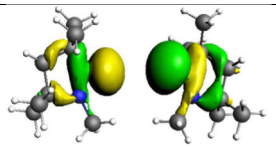 HOMO (ε = -3.58 eV)	 LUMO (ε = -5.10 eV)
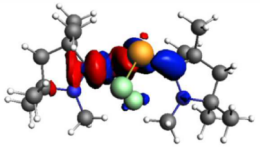 $\Delta\rho_{(2)}$ $\Delta E_{orb(2)}$ = -95.53; $\lvert\nu_{2\alpha}/\nu_{2\beta}\rvert$ = 0.51/0.51	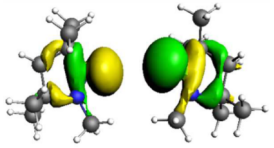 HOMO-1 (ε = -3.89 eV)	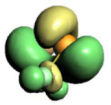 LUMO+1 (ε = -4.21 eV)
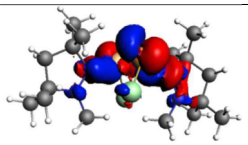 $\Delta\rho_{(3)}$ $\Delta E_{orb(3)}$ = -39.78; $\lvert\nu_{3\alpha}/\nu_{3\beta}\rvert$ = 0.32/0.32	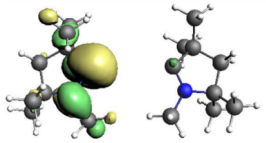 LUMO (ε = -1.06 eV)	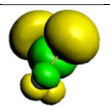 HOMO (ε = -5.25 eV)

Figure 7. Shape of the deformation densities $\Delta\rho_{(1)-(3)}$ that correspond to $\Delta E_{orb(1)-(3)}$ and the associated MOs of cAAC−Si(Cl)Ge(Cl)−cAAC (**1**) and the fragment orbitals of [(cAAC) (cAAC)] and [Si(Cl)Ge(Cl)] in the singlet state (S) at the BP86-D3(BJ)/TZ2P level. The isosurface values are 0.003 au for $\Delta\rho_{(1-2)}$ and 0.001 au for $\Delta\rho_{(3)}$. The eigenvalues $|\nu_n|$ give the size of the charge migration in e. The direction of the charge flow of the deformation densities is red → blue.

cAACSi(Cl)-Ge(Cl)cAAC	cAACSi(Cl) (D)	cAACGe(Cl) (D)
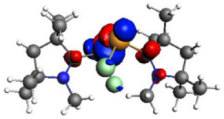 $\Delta\rho_{(1)}$ $\Delta E_{orb(1)}$ = -66.5; $\lvert\nu_{1\alpha}/\nu_{1\beta}\rvert$ = 0.70/0.64	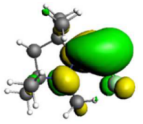 SOMO (ε = -3.53 eV)	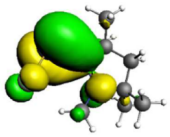 SOMO (ε = -3.73 eV)
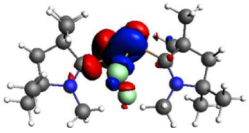 $\Delta\rho_{(2)}$ $\Delta E_{orb(2)}$ = -6.7; $\lvert\nu_{2\alpha}/\nu_{2\beta}\rvert$ = 0.14/0.13	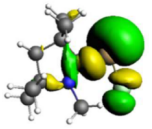 HOMO (ε = -5.03 eV)	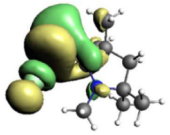 LUMO+1 (ε = -0.82 eV)
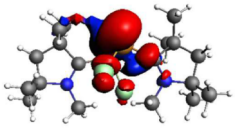 $\Delta\rho_{(3)}$ $\Delta E_{orb(3)}$ = -5.4; $\lvert\nu_{3\alpha}/\nu_{3\beta}\rvert$ = 0.10/0.12	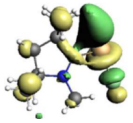 LUMO+2 (ε = -0.41 eV)	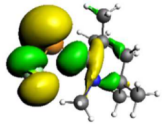 HOMO (ε = -5.48 eV)

Figure 8. Shape of the deformation densities $\Delta\rho_{(1)-(3)}$ that correspond to $\Delta E_{orb(1)-(3)}$ and the associated MOs of cAACSi(Cl)−Ge(Cl)cAAC (**1**) and the fragments orbitals of [cAAC−Si(Cl)] and [cAAC−Ge(Cl)] in the doublet state (D) at the BP86-D3(BJ)/TZ2P level. Isosurface values are 0.003 au for $\Delta\rho_{(1)}$ and 0.0005 au for $\Delta\rho_{(2-3)}$. The eigenvalues $|\nu_n|$ give the size of the charge migration in *e*. The direction of the charge flow of the deformation densities is red → blue. See the Supporting Information for compounds **2**−**7**.

https://doi.org/10.1021/acsomega.4c04196
ACS Omega XXXX, XXX, XXX−XXX

Table 3. EDA-NOCV Analyses of the LSi(Cl)-Ge(Cl)L′ Bond of L−Si(Cl)Ge(Cl)−L′ (1−5) Using [LSi(Cl)] and [L′Ge(Cl)] in the Electronic Doublet (D) States as Interacting Fragments at the BP86-D3(BJ)/TZ2P Level of Theory[a]

energy	interaction	1	2	3	3′	4	5
ΔE_{int}		−53.0	−55.6	−55.3	−56.3	−53.6	−50.1
ΔE_{Pauli}		141.3	142.1	199.6	150.6	136.3	144.9
ΔE_{elstat}[b]		−86.4 (44.4%)	−90.3 (45%)	−126.4 (49.6%)	−99.64 (48.1%)	−87.3 (45.9%)	−91.2 (46.8%)
ΔE_{disp}[b]		−19.9 (10.3%)	−18.4 (9.3%)	−18.8 (7.4%)	−18.1 (8.7%)	−19.2 (10.1%)	−17.5 (9.0%)
ΔE_{orb}[b]		−88.1 (45.3%)	−88.5 (44.9%)	−109.7 (43.0%)	−89.2 (43.1%)	−83.5 (44.0%)	−86.2 (44.2%)
$\Delta E_{orb(1)}$[c]	LSiCl−GeClL′σ electron sharing	−66.5 (75.5%)	−69.2 (78.2%)	−81.8 (74.6%)	−68.6 (76.9%)	−65.7 (78.8%)	−68.4 (79.4%)
$\Delta E_{orb(2)}$[c]	LSi(Cl) → Ge(Cl)L′σ donation	−6.7 (7.7%)	−6.4 (7.2%)	−9.5 (8.7%)	−5.6 (6.2%)	−5.1 (6.1%)	
$\Delta E_{orb(3)}$[c]	LSi(Cl) ← Ge(Cl)L′σ donation	−5.4 (6.1%)			−5.9 (6.7%)	−4.5 (5.4%)	
$\Delta E_{orb(rest)}$		−9.5 (10.7%)	14.5%	16.7%	10.2%	9.8%	20.6%

[a]Energies are in kcal/mol. [b]The values in the parentheses show the contribution to the total attractive interaction $\Delta E_{disp} + \Delta E_{elstat} + \Delta E_{orb}$. [c]The values in the parentheses show the contribution to the total orbital interaction ΔE_{orb}.

Table 4. EDA-NOCV Analyses of the LSi(Cl)−Ge(Cl)L′ Bond of L−Si(Cl)Ge(Cl)−L′ (6−7) Using [LSi(Cl)] and [L′Ge(Cl)] in the Electronic Doublet (D) States as Interacting Fragments and the cAACSi−GecAAC Bond of cAAC−SiGe−cAAC (10) Using [cAACSi] and [cAACGe] in the Electronic Triplet (T) States as Interacting Fragments at the BP86-D3(BJ)/TZ2P Level of Theory[a]

energy	interaction	6	6′	7	Interaction	10
ΔE_{int}		−54.7	−54.7	−56.3		−70.0
ΔE_{Pauli}		177.8	174.8	162.5		178.3
ΔE_{elstat}[b]		−118.8 (51.1%)	−117.6 (51.2%)	−111.2 (50.8%)		−116.0 (46.7%)
ΔE_{disp}[b]		−12.8 (5.5%)	−13.3 (5.8%)	−14.5 (6.5%)		−11.3 (4.6%)
ΔE_{orb}[b]		−100.9 (43.4%)	−98.6 (43.0%)	−93.1 (42.5%)		−120.9 (48.7%)
$\Delta E_{orb(1)}$[c]	LSiCl−GeClL′σ electron sharing	−79.8 (79.1%)	−77.9 (79.0%)	−76.7 (82.4%)	cAACSi−GecAAC σ electron sharing	−64.7 (53.5%)
$\Delta E_{orb(2)}$[c]	LSi(Cl) → Ge(Cl)L′σ donation	−8.5 (8.4%)	−7.1 (7.1%)	−5.9 (6.3%)	cAACSi−GecAAC σ electron sharing	−41.6 (34.4%)
$\Delta E_{orb(3)}$[c]	LSi(Cl) ← Ge(Cl)L′σ donation					
$\Delta E_{orb(rest)}$		12.5%	−13.8%	11.3%		

[a]Energies are in kcal/mol. [b]The values in the parentheses show the contribution to the total attractive interaction $\Delta E_{disp} + \Delta E_{elstat} + \Delta E_{orb}$. [c]The values in the parentheses show the contribution to the total orbital interaction ΔE_{orb}.

charged triplet states, forming electron-sharing σ-bonds and π-dative bonds (Scheme 2, left).

The numerical results of the EDA-NOCV calculations are listed in the Supporting Information. While the BDE values are affected by the geometrical and perhaps the electronic relaxation of the fragments, the absolute value of the interaction energy, ΔE_{int}, is a reliable term for the intrinsic bond strength. Table 2 shows that the highest ΔE_{int} was observed when both of the ligands were cAAC (**1**), and the lowest was observed when both of the ligands were PMe_3 (**7**). The interaction energy ΔE_{int} can be further divided into four terms: ΔE_{Pauli}, ΔE_{ele}, ΔE_{disp}, and ΔE_{orb} (Table 2). The Pauli energy term, ΔE_{Pauli}, in EDA-NOCV corresponds to the energy required to redistribute the electrons in the interacting fragments to remove the electronic overlap caused by the interaction. The highest ΔE_{Pauli} was observed for **1**, where L and L′ were cAAC ligands, the bulkiest among the ligands used in this study. The electrostatic interaction (ΔE_{ele}) contributed approximately 50% of the total attractive forces. The remaining half was contributed by ΔE_{orb} (∼44%) and ΔE_{disp} (∼5%). The smallest absolute value of the orbital term ΔE_{orb} is useful for determining the best bonding description. The EDA-NOCV results show that the best bonding description for compounds **1**−**7** is dative, where the bonding is described by σ- and π-electron-donating dative bonds. ΔE_{orb} can be further divided into the pairwise contributions of the interacting fragments. $\Delta E_{orb(1)}$ (37.1−48.3%) corresponds to the σ-donation from [L L′] to [Si(Cl)Ge(Cl)]. Similar to $\Delta E_{orb(1)}$, $\Delta E_{orb(2)}$ corresponds to σ-donation from [L L′] to [Si(Cl)Ge(Cl)]. The contribution of $\Delta E_{orb(2)}$ (28.4−34.5%) to the total ΔE_{orb} is slightly less than that of $\Delta E_{orb(1)}$. The π backdonation from [Si(Cl)Ge(Cl)] to [L L′] is depicted in $\Delta E_{orb(3)}$, which is less than the overall σ-donation contribution to ΔE_{orb}. A minor contribution of $\Delta E_{orb(4)}$ was found in the **4** (3.7%), **5** (4.1%), and **6** (4.3%) cases (Table 2). The results of EDA-NOCV analyses for the compounds **3′** and **6′** are found to be very similar to those of **3** and **6**, respectively (see the Supporting Information for details).

Figure 7 represents the deformation density plots of compound **1** in which $\Delta\rho_{(1)}$ and $\Delta\rho_{(2)}$ represent the in-phase (++) and out-of-phase (+−) σ-electron donation, respectively, from [cAAC cAAC] to [Si(Cl)Ge(Cl)]. $\Delta\rho_{(3)}$ represents the backdonation from [Si(Cl)Ge(Cl)] to [cAAC cAAC] which contributes 13.7% to the ΔE_{orb}. Similar deformation density plots of compounds **2**−**7** are included in the Supporting Information.

In order to reveal the nature of the bonding interactions between the Si and Ge atoms more accurately, next we performed the EDA-NOCV analysis by cleaving the Si−Ge bonds for **1**−**7** (Figure 8 for **1**, see the Supporting Information for **2**−**7**), generating LSi(Cl) and L′Ge(Cl) fragments (Tables 3 and 4). By changing the charge and spin states of these fragments, we attempted three bonding possibilities. The first possibility involves electron sharing neutral and doublet fragments, whereas the second and third possibilities involve the interaction of singly charged singlet fragments forming

https://doi.org/10.1021/acsomega.4c04196
ACS Omega XXXX, XXX, XXX−XXX

dative bonds (Scheme 2, right). In compounds **1**−**7**, the ΔE_{ele} (44.4−51.2%) contribution to the total attractive forces is slightly higher than the ΔE_{orb} (43.0−45.3%). The remaining contribution is from the dispersive forces, which contribute 5.5−10.3% of the total attractive forces. ΔE_{orb} can be further divided into the pairwise interactions of the fragments. The major contribution to the total ΔE_{orb} comes from the interaction of the unpaired electrons residing in the SOMO of both fragments, which is represented in $\Delta E_{orb(1)}$ (74.6−82.4%). $\Delta E_{orb(2)}$ corresponds to the σ-electron donation from the HOMO of the LSi(Cl) fragment to the vacant orbital of fragment L′Ge(Cl). In some cases, we could observe $\Delta E_{orb(3)}$ corresponding to the σ-electron donation from the HOMO of cAACGe(Cl) fragment to the vacant orbital of fragment cAACSi(Cl). The contribution of $\Delta E_{orb(1)}$ is significantly higher compared to $\Delta E_{orb(2)}$ and $\Delta E_{orb(3)}$ toward ΔE_{orb}. To compare our results with the experimentally isolated homonuclear compound **A**,[4c] the EDA-NOCV calculations have been performed on compound **A** cleaving the bond between the two Si atoms. Our study revealed similar results as of compound **1**, where the best bonding observed between both Si atoms is when the fragments interacted in a neutral doublet state, forming an electron-sharing bond. The major contribution to ΔE_{orb} arises from the interaction of the unpaired electrons in the SOMO of the fragments. It is noticed that the contribution from $\Delta E_{orb(2)}$ and $\Delta E_{orb(3)}$ in **A** (20.5%) is slightly higher than that of **1** (15.8%).

To study the nature of the Si−Ge bonds in compounds **8** and **9**, EDA-NOCV analysis was performed at the BP86/def2-TZV2P level of theory. The bond between Si−Ge of L_2Si−GeL'_2 (L = cAAC; L′ = Cl (**8**), and L = Cl; L′ = cAAC (**9**)) was fragmented creating the fragments $[L_2Si]$ and $[GeL'_2]$. Three different bonding possibilities were tried by changing the charge and spin states of the fragments. The first possibility considered the electron donation from a neutral singlet fragment of $[L_2Si]$ to $[GeL'_2]$ in **8** and $[GeL'_2]$ to $[L_2Si]$ in **9**. In the second case, singly charged doublet fragments were involved creating an electron-sharing bond. The last possibility considered doubly charged singlet fragments involved in electron donation from $[GeL'_2]$ to $[L_2Si]$ in **8** and from $[L_2Si]$ to $[GeL'_2]$ in **9**. Among the three bonding possibilities we have studied, the best bonding was observed when the neutral singlet fragments were involved in the electron donation from the neutral singlet fragment of $[L_2Si]$ to $[GeL'_2]$ in **8** and $[GeL'_2]$ to $[L_2Si]$ in **9**, creating a dative bond (Scheme 3, see the Supporting Information for details).

Scheme 3. Possible Bonding Scenarios Studied for Compounds 8−9

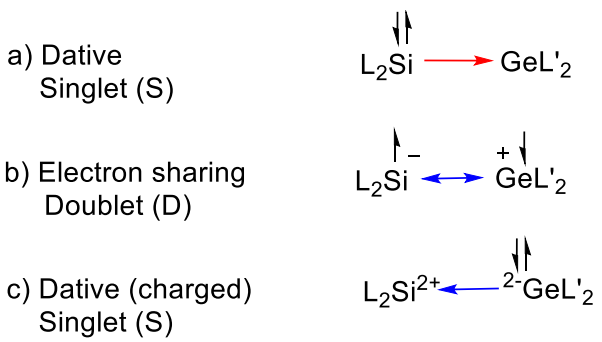

The EDA-NOCV studies were also performed to shed light on the best bonding description of compound **10**, which directed the interaction of the neutral singlet fragments [cAAC cAAC] and [SiGe] to form σ-electron-donating and π-backdonating dative bonds between the Si and Ge atoms (Figure 9). The prior research conducted by Frenking et al.[38,43] extensively examined the bonding and stability of $(L_2)_2E_2$ [L = NHC, cAAC; E = Si, Ge] through EDA-NOCV analyses by cleaving the bonds between the ligands and the central EE backbone. The $(cAAC)_2$ fragment was found to establish two robust dative σ-bonds with the E_2 unit, denoted as [cAAC → E_2 ← cAAC]. Furthermore, there exist two π-bonds (attributed to π-backdonation) between E_2 and $(cAAC)_2$, denoted as [cAAC ← E_2 → cAAC; E = Si, Ge]. The cumulative intrinsic interaction energy is found to be approximately −140 kcal/mol for E = Si and −100 kcal/mol for E = Ge. In the current study, we have observed slightly higher intrinsic interaction energy (−150.31 kcal/mol), which indicates the better stability of the heterodiatomic species, **10**. The major contribution to the orbital interaction is found to be the σ-donation (63.7%) from cAAC ligands to the SiGe moiety ($\Delta E_{orb(1)}$ and $\Delta E_{orb(2)}$) (Figure 9, see the Supporting Information). The strongest interaction comes from the $\Delta E_{orb(1)}$, which represents the σ electron donation in an out-of-phase (+−) combination from HOMO − 1 of [cAAC cAAC] to LUMO of [SiGe]. Slightly weaker σ electron donation in-phase (++) combination is represented in $\Delta E_{orb(2)}$, which is from the HOMO of [cAAC cAAC] to LUMO+1 of [SiGe]. The contribution of π-backdonation is 27.8%, comparatively less than the contribution of σ-donation to the overall ΔE_{orb}. The bond between Si and Ge atoms was cleaved, generating cAACSi and cAACGe fragments (Figure 10, see the Supporting Information). By changing the charge and spin states of these fragments, we attempted two possibilities. The first bonding possibility corresponds to the electron-sharing bond forming from the unpaired electrons from both fragments. The second possibility arises from the interaction of neutral and singlet fragments forming a dative bond. The EDA-NOCV calculations performed on all the bonding possibilities predict that the bonding between Si and Ge is best explained when it is electron-sharing. In compound **10**, ΔE_{orb} (48.7%) contributes slightly greater than ΔE_{ele} (46.7%) to the total attractive forces. Compared to compound **1**, the contribution of ΔE_{disp} decreases to 4.6% in compound **10**. ΔE_{orb} can be divided into $\Delta E_{orb(1)}$ and $\Delta E_{orb(2)}$ corresponding to the pairwise interaction of fragments. $\Delta E_{orb(1)}$ and $\Delta E_{orb(2)}$ show the σ-electron sharing of cAACSi and cAACGe fragments. The contribution of the former is greater compared to that of the latter one (see the Supporting Information). In contrast to **10**, $\Delta E_{orb(1)}$ and $\Delta E_{orb(2)}$ contributed equally to the ΔE_{orb} (42.9% each) in compound **B** ($cAAC_2Si_2$).[4c] Along with the σ-electron-sharing interaction of cAACSi fragments, we also observed a significant amount of σ-donation from the filled orbital to the vacant orbitals of Si ($\Delta E_{orb(3)}$ and $\Delta E_{orb(4)}$; each contributing 6.2%) in **B**. The bonding interactions between Si and Ge atoms are moderately strong (ΔE_{int} = −53 to −70 kcal/mol).

The BDEs of the ligand pair [L, L′] and (Cl)SiGe(Cl) unit Si−Ge of **1**−**7** are in the range of 62−106 kcal/mol following a trend **1** > **2**>**4** > **3** > **5** > **3′** > **6** > **6′** > **7** (Table S3). The lowest binding energy was computed when the ligand pair is $2PMe_3$ in 7, while it is maximum for the cAAC analogue (**1**), suggesting that the stronger π-accepting ability of a pair of

https://doi.org/10.1021/acsomega.4c04196
ACS Omega XXXX, XXX, XXX−XXX

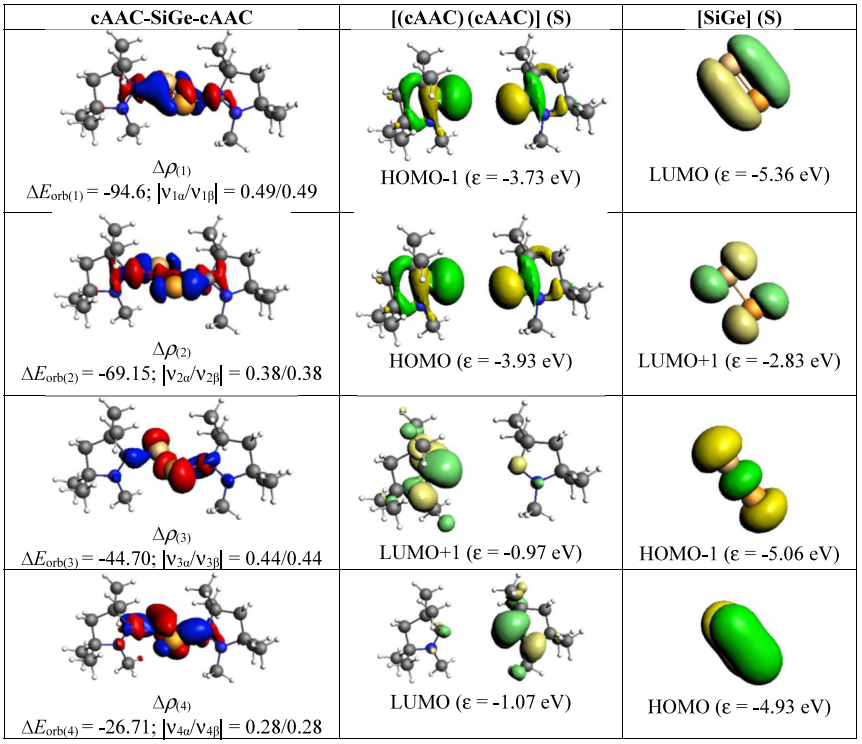

Figure 9. Shape of the deformation densities $\Delta\rho_{(1)-(4)}$ that correspond to $\Delta E_{orb(1)-(4)}$ and the associated MOs of cAAC−SiGe−cAAC (**10**) and the fragments orbitals of [(cAAC) (cAAC)] and [SiGe] in the singlet state (S) at the BP86-D3(BJ)/TZ2P level. The isosurface values are 0.003 au for $\Delta\rho_{(1,3)}$, 0.002 au for $\Delta\rho_{(2)}$, and 0.001 au for $\Delta\rho_{(4)}$. The eigenvalues $|\nu_n|$ give the size of the charge migration in e. The direction of the charge flow of the deformation densities is red → blue.

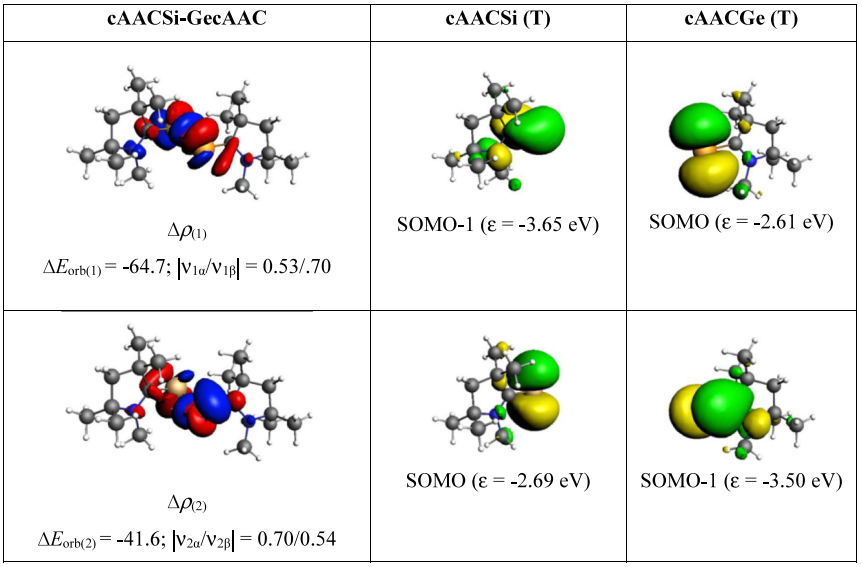

Figure 10. Shape of the deformation densities $\Delta\rho_{(1)-(2)}$ that correspond to $\Delta E_{orb(1)-(2)}$ and the associated MOs of cAACSi−GecAAC (**10**) and the fragments orbitals of [cAAC−Si] and [cAAC−Ge] in the triplet state (T) at the BP86-D3(BJ)/TZ2P level. The isosurface values are 0.0015 au for $\Delta\rho_{(1-2)}$. The eigenvalues $|\nu_n|$ give the size of the charge migration in e. The direction of the charge flow of the deformation densities is red → blue.

cAAC ligands significantly stabilizes [62 (**7**) vs 106 (**1**) kcal/mol] the (Cl)SiGe(Cl) unit in **1**. The trends of BDEs in (cAAC)(Cl)SiGe(Cl)(L′), (NHC)(Cl)SiGe(Cl)(L′), and (Me_3P)(Cl)SiGe(Cl)(L′) are **1** > **2**>**3**, **4** > **5** > **6**, and **3′** > **6′** > **7**, respectively. The cAAC ligand binding to Si (**1**) provides a slightly higher (9 kcal/mol) stabilization energy than the NHC of Si (**4**). The binding in (cAAC)(Cl)SiGe(Cl)(cAAC) (**1**) is more stable by 20 kcal/mol than (NHC)(Cl)SiGe(Cl)(NHC) (**5**), which is even more stable than (Me_3P)(Cl)SiGe(Cl)(Me_3P) (**7**) [**1** > **5** > **7**]. The BDEs of Si−Ge bonds of compounds **1**−**7** and **3′**−**6′** have been given in Table S4, which varies in the range of 48−54 kcal/mol computed with the BP86 functional, suggesting that the central Si−Ge bond is strong enough to be stable at the ambient condition. Hence, it can be predicted that the synthesis of the two cAAC analogue species (**1**) is the most viable among all

https://doi.org/10.1021/acsomega.4c04196
ACS Omega XXXX, XXX, XXX−XXX

(**1**−**7**). Scheme 4 illustrates the comprehensive predicted bonding scenarios for all the hypothesized compounds (**1**−**7**, **10**) assessed through various computational methods. A dative bond exists between [L L′] and [Si(Cl)Ge(Cl)]/fragments, which is formed by the major contribution of σ-electron donation and minor contribution of π-backdonation. It is observed that in compound **10** that the contribution of π-backdonation from [cAAC cAAC] to [SiGe] is greater than the corresponding dihalogenated parent molecule **1**.

Scheme 4. Overall Bonding Scenarios of Compounds 1−7 and 10

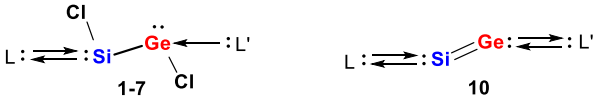

CONCLUSIONS

In conclusion, we have studied the stability and chemical bonding of the heteronuclear 1,2-dichloro-silylene-germylenes **1**−**7** (L)(Cl)SiGe(Cl)(L′) with singly bonded three-coordinate Si and Ge atoms (L, L′ = $cAAC^{Me}$ (**1**); L = $cAAC^{Me}$, L′ = NHC^{Me} (**2**); L = $cAAC^{Me}$, L′ = PMe_3 (**3**); L = PMe_3, L′ = $cAAC^{Me}$ (**3′**); L = NHC^{Me}, L′ = $cAAC^{Me}$ (**4**); L, L′ = NHC^{Me} (**5**); L = NHC^{Me}, L′ = PMe_3 (**6**); L = PMe_3, L′ = NHC^{Me} (**6′**); and L, L′ = PMe_3 (**7**)) along with compounds **8**−**9** with general formula $L_2Si-GeL'_2$ [L = cAAC; L′ = Cl (**8**); and L = Cl; L′ = cAAC (**9**)] and the didehalogenated heteronuclear sila-germene [($cAAC^{Me}$)Si═Ge($cAAC^{Me}$)] (**10**) with multiple bonded two-coordinate Si and Ge atoms in the presence of homo- [L = L′ = $cAAC^{Me}$; NHC^{Me}; and PMe_3] and heterobileptic [L, L′ = $cAAC^{Me}$, NHC^{Me}; $cAAC^{Me}$, PMe_3; and NHC^{Me}, PMe_3] donor base ligands employing NBO, AIM, and EDA-NOCV analyses. The ligand pair [L, L′] is found to be efficiently bound to the central SiGe backbone for **1**−**6** [106−73 kcal/mol]. However, the lowest binding energy (62 kcal/mol) was computed when the ligand pair is two PMe_3 groups (**7**). Among the various ligands probed, cAAC was found to be the most efficient ligand due to its stronger π-accepting ability [106 (**1**) vs 62 (**7**) kcal/mol]. NBO analysis revealed that compound **1** exhibits two bonding occupancies (1.52 and 1.46), and the lone pair of electrons on the Si atom is largely involved in the delocalization over the $C_{cAAC}Si$ atoms in contrast to compounds **2**−**7**, contributing significantly higher stabilization energy in **1**. The larger size and diffused orbitals on Ge permit only the σ-donation from the ligand (L′) to the Ge atom, reflecting the presence of the localized lone pair on it (**1**−**7**). This is also reflected in the single-bond occupancies of the respective bonds and slightly lower WBI compared to the L−Si bond. The EDA-NOCV analyses revealed a deeper understanding of the nature of bonding between the ligand fragments and the central Si(Cl)Ge(Cl) moiety, which is characterized by the dative interaction involving neutral singlet fragments. Further, the division of ΔE_{orb} into the pairwise contributions of the interacting fragments reveal the major contribution to ΔE_{orb} in the form of the σ-donation of ligand fragment to the central Si(Cl)Ge-(Cl) moiety. The nature of the Si−Ge bonds in compounds **1**−**7** is found to be electron sharing by the interaction of neutral doublet-state fragments L(Cl)Si and L(Cl)Ge. The major contribution to ΔE_{orb} is found to be the interaction of the unpaired electron residing in SOMOs of L(Cl)Si and L(Cl)Ge fragments. This contribution marks approximately 80% of the ΔE_{orb}. The remaining contribution comes from the σ donation from Si to Ge (6.1−8.7%) and Ge to Si (5.4−6.7%) fragments. However, the latter is observed only in fewer molecules, e.g., **1** (6.1%), **3′** (6.7%), and **5** (5.4%). The EDA-NOCV and NBO analyses align well with the observation that the extent of π-backdonation from the central Si(Cl)Ge(Cl) backbone to the ligand fragments is minimal (6.5−19.7%). The Si−Ge bond in **8**−**9** is characterized as dative, where electron donation occurs from the atom bonded to the cAAC ligands to the atom bonded to the Cl ligands. The strong electron-donating properties of the cAAC ligands increase the electron density on the atom to which they are attached. This contribution marks 77.0 and 78.1%, respectively, for **8** and **9** to the ΔE_{orb}. The nature of the Si−Ge bond in compound **10** is electron sharing between the neutral triplet-state fragments cAACSi and cAACGe. In this compound, two ΔE_{orb} values are observed ($\Delta E_{orb(1)}$ (53.5%) and $\Delta E_{orb(2)}$ (34.4%)). Both interactions arise from the sharing of electrons residing in the singly occupied orbitals of the fragments in their triplet states. The best bonding scenario of compound **10** is represented by the interaction of neutral singlet fragments [cAAC cAAC] and [SiGe] to form σ-electron-donating and π-backdonating dative bonds.

ASSOCIATED CONTENT

Supporting Information

The Supporting Information is available free of charge at https://pubs.acs.org/doi/10.1021/acsomega.4c04196.

NBO, QTAIM, EDA-NOCV analyses, and optimized coordinates of compounds **1**−**10** (PDF)

Cartesian coordinates of Si−Ge (XYZ)

AUTHOR INFORMATION

Corresponding Author

Sudipta Roy − *Department of Chemistry, Indian Institute of Science Education and Research (IISER) Tirupati, Tirupati 517619 Andhra Pradesh, India;* orcid.org/0000-0002-5883-4329; Email: roy.sudipta@iisertirupati.ac.in

Authors

Maria Francis − *Department of Chemistry, Indian Institute of Science Education and Research (IISER) Tirupati, Tirupati 517619 Andhra Pradesh, India;* orcid.org/0000-0002-0506-4885

Farsana Abdul Salam − *Department of Chemistry, Indian Institute of Science Education and Research (IISER) Tirupati, Tirupati 517619 Andhra Pradesh, India;* orcid.org/0009-0003-2267-3847

Complete contact information is available at: https://pubs.acs.org/10.1021/acsomega.4c04196

Notes

The authors declare no competing financial interest.

ACKNOWLEDGMENTS

S.R. gratefully acknowledges IISER Tirupati for the central computational facility and ANRF-SERB, New Delhi, for the Power Grant (SPG/2021/003237). M.F. thanks CSIR for the SRF.

https://doi.org/10.1021/acsomega.4c04196
ACS Omega XXXX, XXX, XXX−XXX

REFERENCES

(1) Präsang, C.; Scheschkewitz, D. Reactivity in the Periphery of Functionalised Multiple Bonds of Heavier Group 14 Elements. *Chem. Soc. Rev.* **2016**, *45* (4), 900−921.

(2) Rammo, A.; Scheschkewitz, D. Functional Disilenes in Synthesis. *Chem. — Eur. J.* **2018**, *24* (27), 6866−6885.

(3) Fischer, R. C.; Power, P. P. π-Bonding and the Lone Pair Effect in Multiple Bonds Involving Heavier Main Group Elements: Developments in the New Millennium. *Chem. Rev.* **2010**, *110* (7), 3877−3923.

(4) (a) Lee, V. Y.; Sekiguchi, A. Cyclic Polyenes of Heavy Group 14 Elements: New Generation Ligands for Transition-metal Complexes. *Chem. Soc. Rev.* **2008**, *37* (8), 1652−1665. (b) Mondal, K. C.; Roesky, H. W.; Dittrich, B.; Holzmann, N.; Hermann, M.; Frenking, G.; Meents, A. Formation of a 1,4-Diamino-2,3-disila-1,3-butadiene Derivative. *J. Am. Chem. Soc.* **2013**, *135* (43), 15990−15993. (c) Mondal, K. C.; Samuel, P. P.; Roesky, H. W.; Aysin, R. R.; Leites, L. A.; Neudeck, S.; Lübben, J.; Dittrich, B.; Holzmann, N.; Hermann, M.; Frenking, G. One-Electron-Mediated Rearrangements of 2,3-Disiladicarbene. *J. Am. Chem. Soc.* **2014**, *136* (25), 8919−8922. (d) Wang, Y.; Xie, Y.; Wei, P.; King, R. B.; Schaefer, H. F.; von R Schleyer, P.; Robinson, G. H.; Robinson, G. H. A Stable Silicon(0) Compound with a Si = Si Double Bond. *Science* **2008**, *321* (5892), 1069−1071.

(5) Goldberg, D. E.; Harris, D. H.; Lappert, M. F.; Thomas, K. M. A New Synthesis of Divalent Group 4B Alkyls $M[CH(SiMe_3)_2]_2$(M = Ge or Sn), and the Crystal and Molecular and Molecular Strcuture of the Tin Compound. *J. Chem. Soc., Chem. Commun.* **1976**, No. 7, 261−262.

(6) Davidson, P. J.; Harris, D. H.; Lappert, M. F. Subvalent Group 4B Metal Alkyls and Amides. Part I. The Synthesis and Physical Properties of Kinetically Stable Bis[Bis(Trimethysilyl)Methyl]-germanium(II), -tin(II), and -lead(II). *J. Chem. Soc., Dalton Trans.* **1976**, *21*, 2268−2274.

(7) West, R.; Fink, M. J.; Michl, J. Tetramesityldisilene a Stable Compound Containing a Silicon-Silicon Double Bond. *Science* **1981**, *214* (4527), 1343−1344.

(8) Kutzelnigg, W. Chemical Bonding in Higher Main Group Elements. *Angew. Chem., Int. Ed.* **1984**, *23* (4), 272−295.

(9) (a) Stender, M.; Phillips, A. D.; Wright, R. J.; Power, P. P. Synthesis and Characterization of a Digermanium Analogue of an Alkyne. *Angew. Chem., Int. Ed.* **2002**, *41* (10), 1785−1787. (b) Phillips, A. D.; Wright, R. J.; Olmstead, M. M.; Power, P. P. Synthesis and Characterization of 2,6-$Dipp_2$-$H_3C_6SnSnC_6H_3$-2,6-$Dipp_2$ (Dipp = C_6H_3-2,6-Pr^i_2): A Tin Analogue of an Alkyne. *J. Am. Chem. Soc.* **2002**, *124* (21), 5930−5931.

(10) Sekiguchi, A.; Kinjo, R.; Ichinohe, M. A Stable Compound Containing a Silicon-Silicon Triple Bond. *Science* **2004**, *305* (5691), 1755−1757.

(11) Lee, V. Y.; Ichinohe, M.; Sekiguchi, A.; Takagi, N.; Nagase, S. The First Three Membered Unsaturated Rings Consisting of Different Heavier Group 14 Elements: 1-Disilagermirene with a Si = Si Double Bond and Its Isomerization to a 2-Disilagermirene with a Si = Ge Double Bond. *J. Am. Chem. Soc.* **2000**, *122* (37), 9034−9035.

(12) Lee, V. Y.; Ichinohe, M.; Sekiguchi, A. The First Metalladiene of Group 14 Elements with a Silole- Type Structure with Si = Ge and C = C Double Bonds. *J. Am. Chem. Soc.* **2000**, *122* (50), 12604−12605.

(13) Iwamoto, T.; Masuda, H.; Kabuto, C.; Kira, M. Trigermaallene and 1,3-Digermasilaallene. *Organometallics* **2005**, *24* (2), 197−199.

(14) Iwamoto, T.; Abe, T.; Kabuto, C.; Kira, M. A Missing Allene of Heavy Group 14 Elements: 2-germadisilaallene. *Chem. Commun.* **2005**, No. 41, 5190−5192.

(15) Iwamoto, T.; Okita, J.; Yoshida, N.; Kira, M. Structure and Reactions of an Isolable Ge = Si Doubly Bonded Compound, Tetra(*t*-butyldimethylsilyl)Germasilene. *Silicon* **2010**, *2* (4), 209−216.

(16) Igarashi, M.; ıchinohe, M.; Sekiguchi, A. A Stable Silagermene $(^tBu_3Si)_2Si$ = $Ge(Mes)_2$ (Mes = 2,4,6 trimethylphenyl): Synthesis, Xray Crystal Structure, and Thermal Isomerization. *Heteroat. Chem.* **2008**, *19* (7), 649−653.

(17) Ichinohe, M.; Arai, Y.; Sekiguchi, A.; Takagi, N.; Nagase, S. A New Approach to the Synthesis of Unsymmetrical Disilenes and Germasilene: Unusual ^{29}Si NMR Chemical Shifts and Regiospecific Methanol Addition. *Organometallics* **2001**, *20* (20), 4141−4143.

(18) Baines, K. M.; Cooke, J. A. Tetramesitylgermasilene: The First Relatively Stable Germasilene and Its Rearrangement to a Silylgermylene. *Organometallics* **1992**, *11* (11), 3487−3488.

(19) Jana, A.; Huch, V.; Scheschkewitz, D. NHC Stabilized Silagermenylidene: A Heavier Analogue of Vinylidene. *Angew. Chem., Int. Ed.* **2013**, *52* (46), 12179−12182.

(20) Qin, Y.; Zheng, G.; Guo, Y.; Gao, F.; Ma, J.; Sun, W.; Xie, G.; Chen, S.; Wang, Y.; Sun, H.; Li, A.; Wang, W. A Silylene-Germylene Molecule Containing a Si^I-Ge^I Single Bond. *Chem. − Eur. J.* **2020**, *26* (28), 6122−6125.

(21) Arduengo, A. J., III; Harlow, R. L.; Kline, M. A Stable Crystalline Carbene. *J. Am. Chem. Soc.* **1991**, *113* (1), 361−363.

(22) Lavallo, V.; Canac, Y.; Präsang, C.; Donnadieu, B.; Bertrand, G. Stable Cyclic (Alkyl)(Amino)Carbenes as Rigid or Flexible, Bulky, Electron-Rich Ligands for Transition-Metal Catalysts: A Quaternary Carbon Atom Makes the Difference. *Angew. Chem., Int. Ed.* **2005**, *44* (35), 5705−5709.

(23) Becke, A. D. Density-Functional Exchange-Energy Approximation with Correct Asymptotic Behavior. *Phys. Rev. A: At., Mol., Opt. Phys.* **1988**, *38* (6), 3098−3100.

(24) Frisch, M. J.; Trucks, G. W.; Schlegel, H. B.; Scuseria, G. E.; Robb, M. A.; Cheeseman, J. R.; Scalmani, G.; Barone, V.; Petersson, G. A.; Nakatsuji, H.; Li, X.; Caricato, M.; Marenich, A. V.; Bloino, J.; Janesko, B. G.; Gomperts, R.; Mennucci, B.; Hratchian, H. P.; Ortiz, J. V.; Izmaylov, A. F.; Sonnenberg, J. L.; Williams-Young, D.; Ding, F.; Lipparini, F.; Egidi, F.; Goings, J.; Peng, B.; Petrone, A.; Henderson, T.; Ranasinghe, D.; Zakrzewski, V. G.; Gao, J.; Rega, N.; Zheng, G.; Liang, W.; Hada, M.; Ehara, M.; Toyota, K.; Fukuda, R.; Hasegawa, J.; Ishida, M.; Nakajima, T.; Honda, Y.; Kitao, O.; Nakai, H.; Vreven, T.; Throssell, K.; Montgomery, J. A., Jr.; Peralta, J. E.; Ogliaro, F.; Bearpark, M. J.; Heyd, J. J.; Brothers, E. N.; Kudin, K. N.; Staroverov, V. N.; Keith, T. A.; Kobayashi, R.; Normand, J.; Raghavachari, K.; Rendell, A. P.; Burant, J. C.; Iyengar, S. S.; Tomasi, J.; Cossi, M.; Millam, J. M.; Klene, M.; Adamo, C.; Cammi, R.; Ochterski, J. W.; Martin, R. L.; Morokuma, K.; Farkas, O.; Foresman, J. B.; Fox, D. J. *Gaussian, 09*, Revision, A.02.; Gaussian, Inc.: Wallingford CT, 2016.

(25) Wiberg, K. B. Application of the Poplesantrysegal CNDO Method to the Cyclopropylcarbinyl and Cyclobutyl Cation and to Bicyclobutane. *Tetrahedron* **1968**, *24* (3), 1083−1096.

(26) (a) Landis, C. R.; Weinhold, F. Frontmatter. In *Valency and Bonding: A Natural Bond Orbital Donor Acceptor Perspective*; Cambridge University Press: Cambridge, 2005; p iiv. (b) Reed, A. E.; Curtiss, L. A.; Weinhold, F. Intermolecular Interactions from a Natural Bond Orbital, Donor acceptor Viewpoint. *Chem. Rev.* **1988**, *88* (6), 899−926. (c) Reed, A. E.; Weinstock, R. B.; Weinhold, F. Natural Population Analysis. *J. Chem. Phys.* **1985**, *83* (2), 735−746. (d) Landis, C. R.; Weinhold, F. The NBO View of Chemical Bonding. In *The Chemical Bond*, 2014; p 91120.

(27) (a) Bader, R. F. W. *Atoms in Molecules: A Quantum Theory*; Oxford University Press: USA, 1994. (b) Bader, R. F. W. A Quantum Theory of Molecular Structure and Its Applications. *Chem. Rev.* **1991**, *91*, 893−928. (c) Bader, R. F. W. Atoms in Molecules. *Acc. Chem. Res.* **1985**, *18*, 9. (d) Matta, C. F.; Boyd, R. J. *The Quantum Theory of Atoms in Molecules*; Wiley VCH, 2007.

(28) (a) SCM. *ADF2020.102, Theoretical Chemistry*; Vrije Universiteit: 782 Amsterdam, The Netherlands http://www.scm.com (accessed Jan 15, 2021). (b) Ziegler, T.; Rauk, A. On the calculation of bonding energies by the Hartree Fock Slater method. *Theor. Chim. Acta* **1977**, *46*, 1−10. (c) Morokuma, K. Molecular Orbital Studies of Hydrogen Bonds. III. C = O···H−O Hydrogen Bond in H_2CO···H_2O and H_2CO···$2H_2O$. *J. Chem. Phys.* **1971**, *55* (3), 1236−1244. (d) te Velde, G.; Bickelhaupt, F. M.; Baerends, E. J.; Fonseca Guerra, C.; van Gisbergen, S. J. A.; Snijders, J. G.; Ziegler, T.

https://doi.org/10.1021/acsomega.4c04196
ACS Omega XXXX, XXX, XXX−XXX

Chemistry with ADF. *J. Comput. Chem.* **2001**, *22* (9), 931−967. (e) Mitoraj, M.; Michalak, A. Donor-Acceptor Properties of Ligands from the Natural Orbitals for Chemical Valence. *Organometallics* **2007**, *26*, 6576−6580. (f) Mitoraj, M.; Michalak, A. Applications of natural orbitals for chemical valence in a description of bonding in conjugated molecules. *J. Mol. Model.* **2008**, *14*, 681−687. (g) Mitoraj, M. P.; Michalak, A.; Ziegler, T. A Combined Charge and Energy Decomposition Scheme for Bond Analysis. *J. Chem. Theory Comput.* **2009**, *5* (4), 962−975. (h) Michalak, A.; Mitoraj, M.; Ziegler, T. Bond Orbitals from Chemical Valence Theory. *J. Phys. Chem. A* **2008**, *112* (9), 1933−1939. (i) Ziegler, T.; Rauk, A. Carbon Monoxide, Carbon Monosulfide, Molecular Nitrogen, Phosphorus Trifluoride, and Methyl Isocyanide as σ Donors and π. Acceptors. A Theoretical Study by the Hartree-Fock-Slater Transition-state Method. *Inorg. Chem.* **1979**, *18* (7), 1755−1759. (j) van Lenthe, E.; Baerends, E. J.; Snijders, J. G. Relativistic Regular Two-Component Hamiltonians. *J. Chem. Phys.* **1993**, *99* (6), 4597−4610.

(29) Janiak, C. A Critical Account on $\pi-\pi$ Stacking in Metal Complexes with Aromatic Nitrogen-containing Ligands. *J. Chem. Soc., Dalton Trans.* **2000**, *21*, 3885−3896.

(30) Mohapatra, C.; Kundu, S.; Paesch, A. N.; Herbst-Irmer, R.; Stalke, D.; Andrada, D. M.; Frenking, G.; Roesky, H. W. The Structure of the Carbene Stabilized Si_2H_2 May Be Equally Well Described with Coordinate Bonds as with Classical Double Bonds. *J. Am. Chem. Soc.* **2016**, *138* (33), 10429−10432.

(31) Kundu, S.; Samuel, P. P.; Luebben, A.; Andrada, D. M.; Frenking, G.; Dittrich, B.; Roesky, H. W. Carbene Stabilized Interconnected Bis-Germylene and Its Silicon Analogue with Small Methyl Substituents. *Dalton Trans.* **2017**, *46* (24), 7947−7952.

(32) Ghadwal, R. S.; Roesky, H. W.; Merkel, S.; Henn, J.; Stalke, D. Lewis Base Stabilized Dichlorosilylene. *Angew. Chem., Int. Ed.* **2009**, *48* (31), 5683−5686.

(33) Liu, Y.; Keil, H.; Yang, Z.; Herbst-Irmer, R.; Roesky, H. W.; Stalke, D. Phosphorus Silicon Compounds from the Reduction of $MesP(H)SiCl_2Ph$/Carbene with and without Metal. *Eur. J. Inorg. Chem.* **2020**, *2020* (23), 2273−2278.

(34) Hansen, K.; Szilvási, T.; Blom, B.; Irran, E.; Driess, M. A Donor-Stabilized Zwitterionic "Half-Parent" Phosphasilene and Its Unusual Reactivity towards Small Molecules. *Chem.—Eur. J.* **2014**, *20* (7), 1947−1956.

(35) Siddiqui, M. M.; Sarkar, S. K.; Sinhababu, S.; Ruth, P. N.; Herbst-Irmer, R.; Stalke, D.; Ghosh, M.; Fu, M.; Zhao, L.; Casanova, D.; Frenking, G.; Schwederski, B.; Kaim, W.; Roesky, H. W. Isolation of Transient Acyclic Germanium(I) Radicals Stabilized by Cyclic Alkyl(Amino) Carbenes. *J. Am. Chem. Soc.* **2019**, *141* (5), 1908−1912.

(36) Li, Y.; Mondal, K. C.; Roesky, H. W.; Zhu, H.; Stollberg, P.; HerbstIrmer, R.; Stalke, D.; Andrada, D. M. Acyclic Germylones: Congeners of Allenes with a Central Germanium Atom. *J. Am. Chem. Soc.* **2013**, *135* (33), 12422−12428.

(37) Nag, E.; Francis, M.; Battuluri, S.; Sinu, B. B.; Roy, S. Isolation of Elusive PhosphinideneChlorotetrylenes: The Heavier Cyanogen Chloride Analogues. *Chem. − Eur. J.* **2022**, *28* (54), No. e202201242.

(38) Sidiropoulos, A.; Jones, C.; Stasch, A.; Klein, S.; Frenking, G. N. Heterocyclic Carbene Stabilized Digermanium(0). *Angew. Chem., Int. Ed.* **2009**, *48* (51), 9701−9704.

(39) Izod, K.; Rayner, D. G.; El-Hamruni, S. M.; Harrington, R. W.; Baisch, U. Stabilization of a Diphosphagermylene through $p\pi$-$p\pi$ Interactions with a Trigonal-Planar Phosphorus Center. *Angew. Chem., Int. Ed.* **2014**, *53* (14), 3636−3640.

(40) Yao, S.; Brym, M.; Merz, K.; Driess, M. Facile Access to a Stable Divalent Germanium Compound with a Terminal PH_2 Group and Related PR_2 Derivatives. *Organometallics* **2008**, *27* (14), 3601−3607.

(41) Majhi, P. K.; Huch, V.; Scheschkewitz, D. A Mixed Heavier Si = Ge Analogue of a Vinyl Anion. *Angew. Chem., Int. Ed.* **2021**, *60* (1), 242−246.

(42) Majhi, P. K.; Zimmer, M.; Morgenstern, B.; Scheschkewitz, D. Transition-Metal Complexes of Heavier Cyclopropenes: Non-Dewar−Chatt−Duncanson Coordination and Facile Si=Ge Functionalization. *J. Am. Chem. Soc.* **2021**, *143* (24), 8981−8986.

(43) Holzmann, N.; Andrada, D. M.; Frenking, G. Bonding Situation in Silicon Complexes $[(L)_2(Si_2)]$ and $[(L)_2(Si)]$ with NHC and CAAC Ligands. *J. Organomet. Chem.* **2015**, *792*, 139−148.

https://doi.org/10.1021/acsomega.4c04196
ACS Omega XXXX, XXX, XXX−XXX